UNIVERSITY OF CALIFORNIA,
IRVINE

The influence of mechanical stress on the growth and remodeling of a tumor

THESIS

submitted in partial satisfaction of the requirements
for the degree of

MASTER OF MATHEMATICAL, COMPUTATIONAL & SYSTEMS BIOLOGY (MCSB)

in Center for Complex Biological Systems

by

Jihye Choi

Thesis Committee:
Chancellor's Professor John Lowengrub, Chair
Professor Long Chen
Associate Professor Jun Allard

2019

TABLE OF CONTENTS

LIST OF FIGURES

LIST OF TABLES

ACKNOWLEDGMENTS

In the beginning, I would like to express my sincere appreciation to my advisor, Professor Lowengrub, who continuously support my Master study and research with his patience, enthusiasm, and extensive knowledge. He guided me throughout entire process of researching and writing this thesis with invaluable advice and patience. This work would not have been possible without his precious help. I could not have imagined having a better mentor for my Master study.

Besides my advisor, my deepest gratitude also goes to my thesis committee members, Professor Jun Allard and Professor Long Chen, for their great support, encouragement, and insightful comments.

Last but not the least, I would like to thank my beloved family for supporting me both financially and emotionally throughout my life. Their love, encouragement, and support helped me in completion of this paper.

ABSTRACT OF THE THESIS

The influence of mechanical stress on the growth and remodeling of a tumor

By

Jihye Choi

Literature M.S. Thesis

Mathematical, Computational and Systems Biology

University of California, Irvine, 2019

Professor Lowengrub, Chair

Mechanical forces are generated during tumor growth and progression. Numerous studies have investigated the effect of mechanical stress on cell behaviors, but there is still much to be understood. Many experimental and theoretical studies have investigated the effect of mechanical forces using multicellular tumor spheroids (MCTSs) as models of pre-vascular tumor growth. Here, we review two theoretical studies. In the first, "Influence of the mechanical properties of the necrotic core on the growth and remodeling of tumour spheroids," Giverso and Preziosi (2019) [1] develop a mathematical model to study the growth and remodeling of a MCTS with a necrotic core, which is composed of either calcified debris or a liquid cavity. In the second, "An avascular tumor growth model based on porous media mechanics and evolving natural states," Mascheroni et al. (2018) [2] analyze the influence of the microenvironment on tumor growth and remodeling.

CHAPTER 1: INTRODUCTION

A solid tumor is an abnormal mass of tissue that is composed of cancer cells and different types of host cells, and extracellular matrix (ECM). Solid stress (force applied to a unit area) accumulates in both the tumor interior and in the microenvironment surrounding the tumor. Stresses can be divided into two categories: growth-induced (or residual) stress and externally applied stress [3, 4]. The former develops when the proliferating cancer cells strain the tumor microenvironment, which contributes reciprocal forces and deforms the adjacent normal tissue. The latter is generated by the mechanical interactions between a growing tumor and the host tissue. When the growing tumor applies forces to the nearby normal tissue, the tissue exerts reciprocal compressive stresses to the tumor to resist tumor expansion. The solid stress, which can generate both compression and expansion of a material, influences cell proliferation and tissue remodeling.

Numerous studies have been done to explore the influence of mechanical stress on cell behavior (e.g., [5-10]). For example, Helmlinger and coworkers [8] found experimentally that in a variety of tumor types compressive stress inhibits proliferation of multicellular tumor spheroids (MCTS). Many mathematical models of MCTS have also been developed (e.g., [5, 6, 10, 11]). However, developing mathematical models of stress generation during tumor growth is challenging because unlike classical continuum mechanics applications where mass is conserved, in the tumor growth context the amount of solid mass increases because of cell proliferation. In addition, stresses can induce plastic re-arrangements of structural materials (e.g., ECM, intracellular, and cell motion) that relax the overall stress [12, 13].

Starting with the work of Rodriguez et al. (1994) and Skalak at el. (1996) [14, 15], the effects of growth and re-arrangements have been incorporated through a multiplicative decomposition of the deformation gradient tensor. In particular, the deformation is a change in shape caused by an applied load, and it can be divided into three categories: elastic, plastic, and anelastic deformation [16]. Elastic deformation is a temporary shape change that is self-reversing upon the removal of the external load. In other words, the shape can be changed with low stress but is recoverable when the load is removed. On the other hand, a plastic deformation is a permanent shape change caused by the external load (high stress) which is irreversible. Here, we focus on plastic deformations generated by cell or tissue remodeling. Lastly, anelastic deformation refers to a distortion that is not elastic, and here we focus on anelastic deformations generated by growth of cells or tissues.

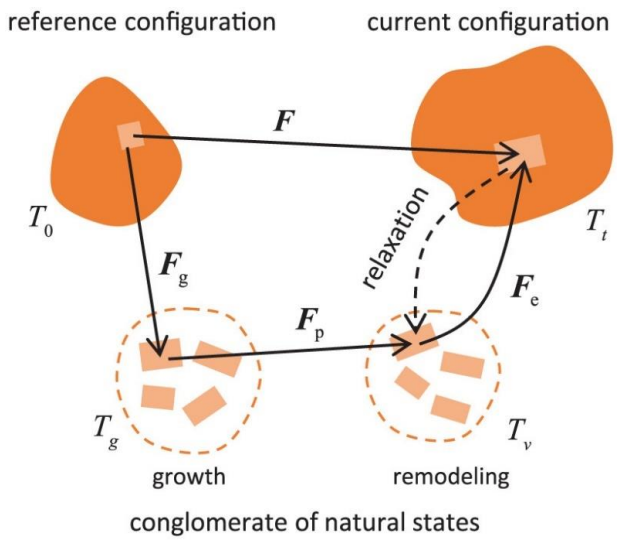

Figure 1. A diagram that represents the multiplicative decomposition of the deformation gradient tensor [2].

Following [14, 15], the deformation gradient can be written as

$$F = F_e F_a = F_e F_p F_g, \qquad (1)$$

where F_e is the elastic deformation tensor, F_p is the plastic deformation tensor, and F_g is the anelastic deformation tensor generated by tumor growth (e.g., mass gain or loss). F_g maps vectors in the reference configuration T_0 into vectors in the growth configuration T_g, and F_p maps vectors in the T_g into vectors in the natural (or a locally relaxed) configuration T_v (Figure 1) [1, 2]. The natural configuration refers to a configuration where a body can exist in the absence of external stress through a rigid body motion [17, 18].

To explore the influence of mechanical factors on tumor growth and remodeling, Giverso and Preziosi (2019) and Mascheroni et al. (2017) [1, 2] develop mathematical models of MCTS as a model system because MCTS are much simpler to model than in vivo tumors but nevertheless exhibit many features of in vivo growth, such as three-dimensional, nutrient-limited growth and stress generation. As such, MCTS also provide a good model of the early, avascular stage of in vivo tumor growth [19, 20]. In these papers, which we review in this thesis, MCTS are modeled as a porous medium composed of solid and liquid phases. The models aim to describe the growth and remodeling caused by mechanical and biochemical stimuli, through the multiplicative decomposition of the deformation gradient tensor, balance laws with diffusion-reaction equations, and a system of ordinary differential equations. Giverso et al. utilize this framework to investigate how a necrotic core of MCTS mechanically influences its growth and remodeling, while Mascheroni et al. study tumors grown in two different environments—a culture medium (MCTS), as well as two in vivo configurations—in order to investigate how the mechanical properties of the microenvironment influence tumor growth and remodeling.

This paper is organized as follows: in Chapter 2, we review the article, “Influence of the mechanical properties of the necrotic core on the growth and remodeling of tumour

spheroids" by Giverso and Preziosi. In Chapter 3, we review the article, "An avascular tumor growth model based on porous media mechanics and evolving natural states" by Mascheroni et al. Finally, we discuss connections between these two articles and future studies in Chapter 4.

CHAPTER 2:

Survey of "Influence of the mechanical properties of the necrotic core on the growth and remodelling of tumour spheroids" by Giverso and Preziosi

In the article, "Influence of the mechanical properties of the necrotic core on the growth and remodeling of tumour spheroids", Giverso et al. [1] propose a mathematical model for the mechanical behavior of MCTS, whose growth is directly related to the nutrient diffusion from the external environment and as such, MCTS describe the early, prevascular stages of in vivo tumor growth [20].

In [1], the authors model avascular multicellular tumor spheroids as three concentric layers: (i) an inner necrotic core, where cells have died due to lack of nutrients, which must diffuse in from the surrounding medium; (ii) a shell of quiescent cells, where there are sufficient levels of nutrients to keep the cells alive but not enough to enable them to proliferate; and (iii) an outermost proliferative ring, where cells have enough nutrients to divide (Figure 2) [21-23].

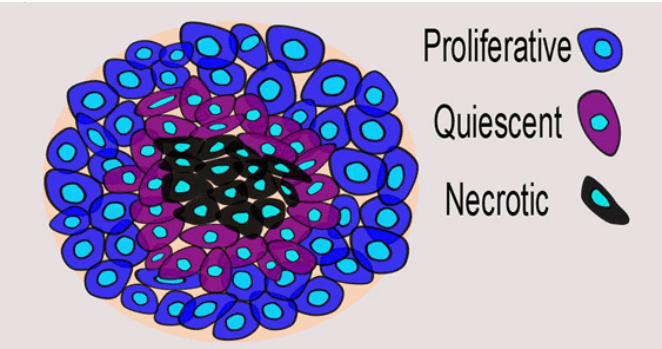

Figure 2. Geometry of a MCTS with three layers: a necrotic core (black), a quiescent region (purple), and a proliferative ring (blue) [24].

Quiescent cells can undergo both apoptosis (programmed cell death) and necrosis--premature cell death by external factors such as nutrient deprivation and hypoxia. In

contrast to apoptotic cells, which could occur anywhere in the MCTS, necrotic cells primarily occur in the nutrient-poor inner core in a MCTS [25-27]. In addition, necrotic cells can swell up to several times their initial volume by osmosis and then undergo lysis by fluid or protein leakage [26, 27]. The necrotic core in a MCTS can be either composed of a liquid cavity or calcified debris [27-29]. In the former case, necrotic cells dissolve, and their debris is removed from the system, forming a cavity filled by liquid. In the latter case, the necrotic core undergoes dystrophic calcification due to cell death. Therefore, the boundaries between each layer may change as time passes although in [1], the size of the rigid necrotic region is fixed. The novel feature of the model [1], compared to other models in the literature, is that it includes the effect of the mechanical response of the necrotic core.

In [1], a multiphase model is developed that treats the tumor as a mixture of solid tissue (proliferating and quiescent cells) and interstitial liquid, which transfers the nutrients from the external environment to the spheroid. The authors also assume that the solid tumor develops symmetrically during its entire progression, rather than asymmetrically or into complex shapes. Therefore, the mathematical model consists of a system of ordinary differential equations, generated by mass and momentum conservation, and a reaction-diffusion equation, describing the transport of nutrients within the tumor.

In [1], the tumor is described as a mixture characterized by a solid fraction ϕ_s and a liquid fraction ϕ_f, and the saturation condition for the spheroid is

$$\phi_s + \phi_f = 1. \tag{2}$$

Then the mass balance laws of the solid and the fluid phases of the spheroid are

$$(J\dot{\phi}_s) = J\phi_s\Gamma^s, \tag{3}$$

$$(J\dot{\phi}_f) + \mathrm{Div}\left(J\phi_f F^{-1}(v_f - v_s)\right) = 0, \tag{4}$$

where the overdots denote the time derivatives, Γ^s is the net rate of mass gain (e.g., cell division/death), and J is volumetric change of the solid phase, where $J = J_e J_p J_g$ [30]. Here, $J_e = \det(F_e)$ represents the volume changes of the solid phase induced by the elastic deformation, whereas $J_g = \det(F_g)$ refers to the volume increase due to growth and J_p is the volume change due to the plastic deformations. The operator $\mathrm{Div}(\cdot)$ describes the divergence in material coordinates. In [1], it is assumed that $J_p = \det(F_p) = 1$, which implies that $J = J_e J_g$. Further, v_f and v_s are the velocities of the fluid and solid phases. Since $J_g = J/J_e = J\phi_s/\phi_{sn}$, where $\phi_{sn} \coloneqq J_e\phi_s$ is the mass density of the solid phase calculated with respect to the natural configuration, then

$$\phi_s = \frac{\phi_{sn}}{J_e} = \phi_{sn}\frac{J_g}{J}. \tag{5}$$

Assuming Darcy's law [31], the fluid flow changes based on the permeability of the medium (K) and the interstitial pressure (p) gradient

$$\nu\varphi^f(v_f - v_s) = -\mathbf{K}(\phi_s)\,\mathrm{grad}\,(p), \tag{6}$$

where ν is the viscosity of the fluid phase and $\mathbf{K}(\phi_s)$ is the permeability of the medium. In material coordinates, $\mathrm{grad}\,(p) = F^{-T}\mathrm{Grad}\,(p)$,

$$j = \frac{1}{\nu}\,\mathrm{Div}\left(JF^{-1}KF^{-T}\mathrm{Grad}(p)\right). \tag{7}$$

Furthermore, by neglecting external body forces, the balance laws of momentum for the biphasic model become

$$\mathrm{Div}\,(\sigma^s + \sigma^f) = 0, \tag{8}$$

and the closure condition with respect to the momentum exchange rate (m) is $m^s + m^f = 0$ [2]. Here, $\sigma^s \coloneqq JT_sF^{-T}$ and $\sigma^f \coloneqq JT_fF^{-T}$ are the elastic stress tensors of the solid and

the liquid phases, respectively, which are defined by the standard Piola transformation. T_s refers to the Cauchy stress tensor of the solid phase, which is used to analyze a material body that experiences elastic deformations. To simulate tumor remodeling, [15] derive the plastic stress tensor, T_p, and the plastic deformation rate, L_p, by modifying the model presented in [32]:

$$T_p = F_e^T T'_s F_e^{-T}, \tag{9}$$

$$L_p = \frac{J}{2\eta(\phi_s)}\left[1 - \frac{\tau(\phi_s)}{f(T'_s)}\right]_+ \text{sym}\,(F_e^T T'_s F_e^{-T}). \tag{10}$$

$[\cdot]_+$ is the positive part of its argument, and T'_s indicates the deviatoric part of the stress tensor of the solid phase. The deviatoric stress refers to a stress that tends to alter the shape of a material, i.e. body distortion [33]. $\tau(\phi_s)$ is the yield stress, and $f(T'_s)$ refers to "the set frame invariant measure of the stress" of the solid phase.

To find the relation between Γ^s and J_g, Ambrosi et al. (2009) [34] differentiate $J_e = \det(F_e)$ and $J = J_g J_e$ with respect to t to get

$$\frac{d}{dt}\log(\phi_s J_e) = 0, \text{ and} \tag{11}$$

$$\frac{1}{J}\frac{dJ}{dt} = \frac{1}{J_g}\frac{dJ_g}{dt} + \frac{1}{J_e}\frac{dJ_e}{dt} \tag{12}$$

Therefore, the latter equation can be rewritten as

$$\frac{1}{J_g}\frac{dJ_g}{dt} = \frac{1}{\phi_s}\left(\frac{d\phi_s}{dt} + \frac{\phi_s}{J}\frac{dJ}{dt}\right). \tag{13}$$

From this equation and the mass balance equation for the solid phase, one obtains

$$\frac{\dot{J_g}}{J_g} = \Gamma^s \tag{14}$$

and the proliferation and death of cells inside a MCTS are assumed to be regulated by nutrients, which are transported from a culture medium to the spheroid by advection and

diffusion. Since cells are assumed to proliferate only if the nutrient concentration (c_n) is above a threshold (c_{n0}), i.e. $c_n > c_{n0}$, the growth rate is taken to be [15]

$$\Gamma^s = \gamma_s(\phi_{max} - \phi_s)(c_n - c_{n0})_+. \quad (15)$$

Therefore, the mass balance law for nutrients in the liquid phase becomes [35]

$$\dot{c_n} = \frac{1}{\nu\phi_f}(F^{-1}\mathbf{K}(\phi_s)F^{-T}\text{Grad}\, p)\cdot\text{Grad}\, c_n + \frac{1}{J\phi_f}\text{Div}(JF^{-1}D_nF^{-T}\text{Grad}\, c_n) - \zeta\frac{\phi_s}{\phi_f}c_n \quad (16)$$

where c_n is the nutrient concentration, ζ is the rate of nutrient consumption, and D_n is the diffusion coefficient The overdot represents the time derivative, and $\text{Grad}(\cdot)$ and $\text{Div}(\cdot)$ are the gradient and divergence in the material coordinates, respectively.

Because the MCTS is assumed to grow symmetrically, the above model can be simplified using spherical coordinates, (R, Θ, Φ):

$$r(t,X) = \chi(t,R), \quad \vartheta(t,X) = \Theta, \quad \varphi(t,X) = \Phi. \quad (17)$$

By using the equations (Eqn. (5)-(8), (10), (14), (16)), and by setting the initial radius of a spheroid as $R = R_{out}$ and the radius of its calcified core as R_0, [15] derive the system of equations,

$$\dot{J} = \frac{1}{\nu}\frac{\chi 2}{R^2}\frac{\partial}{\partial R}(K(\phi_s)\Pi^R) + 2\frac{K(\phi_s)}{\nu}\frac{J}{\chi}\Pi^R, \quad (18)$$

$$\dot{g} = \frac{\gamma_s}{3}(\phi_{max} - \phi_s)(c_n - c_{n0})_+ g,. \quad (19)$$

$$\dot{\Psi}_P = -\frac{J\varphi^s}{6\lambda}\left[\left|\frac{J^2\Psi_p^6 - \chi 6}{g^2\Psi_p^2\chi^4} - \frac{2\tau}{\mu\varphi^s}\right|\right]_+ \text{sign}\left(J^2\Psi_p^6 - \chi^6\right)\Psi_P \quad (20)$$

$$\dot{c_n} = \frac{1}{\nu}\frac{\chi^2}{J\phi_f R^2}K(\phi_s)\Pi^R\frac{\partial c_n}{\partial R} + \frac{D_n}{J(1-\phi_s)R^2}\frac{\partial}{\partial R}\left(\frac{\chi^4}{JR^2}\frac{\partial c_n}{\partial R}\right) - \zeta\frac{\phi_s}{\phi_f}c_n, \quad (21)$$

which hold for $R_0 < R < R_{out}$. The tensor $\mathbf{K} = K(\phi_s)I$, and Π^R is the "radial component of the material gradient of pressure pulled-forward to the actual configuration". Π^R can be defined as

$$\Pi^R = \frac{1}{J}\left[\frac{\partial}{\partial R}(P_s^*)^{rR}\right] + \frac{2}{R}\left((P_s^*)^{rR} - (P_s^*)^{\vartheta\Theta}\right), \tag{22}$$

where P_s^* is the constitutive part of the first Piola-Kirchoff stress tensor of the solid phase. The first Piola–Kirchhoff stress tensor relates a force vector in the current configuration to an area vector in the reference configuration [36]. g represents growth amplitude, and γ_s is the growth rate. $\phi_{\max}$ is the maximum cellular volume fraction, and Ψ_P is the measure of tumor remodeling. τ is the remodeling threshold, and λ is defined as the intracellular reorganization time. This system should be solved with the following condition,

$$\frac{\partial}{\partial R}\chi = J\frac{R^2}{\chi^2}, \tag{23}$$

coupled with initial conditions,

$$J(0,R) = 1 \tag{24}$$

$$\Psi_P(0,R) = R, \tag{25}$$

$$g(0,R) = 1 \tag{26}$$

$$c_n(0,R) = e^{-(R-R_{out})^2/\epsilon^2}, \tag{27}$$

and boundary conditions,

$$c_n\big(t,\chi(t,R_{out})\big) = c_b \tag{28}$$

$$(T_s^*)^{rr}\big(t,\chi(R_{out})\big) = P_{appl}(t) \tag{29}$$

$$\chi(t,R_0) = R_0 \tag{30}$$

$$\Pi^R(t,R_0) = 0 \tag{31}$$

$$\frac{\partial c_n}{\partial R}(t,R_0) = 0 \tag{32}$$

$$\dot{\chi}(t,R_0) = v_s^R \Rightarrow \dot{\chi}(t,R_0) = \frac{K(\phi_s)}{\nu}\Pi^R \tag{33}$$

$$T_m^{rr}\big(t,\chi(t,R_0)\big) = T_f^{rr}\big(t,\chi(t,R_0)\big) \Rightarrow (T_s^*)^{rr}\big(t,\chi(t,R_0)\big) = 0 \tag{34}$$

$$\frac{\partial c_n}{\partial R}(t, R_0) = 0. \quad (35)$$

At the external boundary of a MCTS, R_{out}, the concentration of nutrients, c_n, should equal to c_b, the nutrient concentration in the microenvironment (Eqn. (28)) and the radial stress at the outer boundary of the MCTS should be equal to the applied stress, $P_{appl}(t)$, (Eqn. (29)).

Eqns. (30)-(32) describe the requirements that need to be fulfilled by a MCTS with a calcified core at the inner boundary of the spheroid, R_0. Since necrosis takes longer than tumor growth and remodeling, the inner boundary should be fixed (Eqn. (30)). The velocities of the fluid and of solid phases are required to be 0 because the authors assume that the rigid necrotic core is impervious (Eqn. (31)). Furthermore, nutrients cannot pass through the calcified core (Eqn. (32)). On the other hand, Eqn. (33)-(35) are the boundary conditions that need to be satisfied by a tumor spheroid with a liquid core. The inner boundary of a MCTS with a necrotic core is permeable and is not fixed. The flux at the inner boundary is maintained constant, and this boundary changes based on cell volumetric fraction (Eqn. (33)). The radial stress applied by the mixture, T_m^{rr}, equals to the liquid core radial stress, T_f^{rr}" (Eqn. (34)). Finally, the nutrient concentration inside the spheroid's liquid core is null (Eqn. (35)).

In [1], the system is nondimensionalized. Spatial parameters become dimensionless with respect to the initial external radius of the spheroid, R_{out}, whereas temporal parameters nondimensionalized with respect to the typical cell proliferation time, $t_r = (\phi_{max}\gamma_s c_b)^{-1}$. Furthermore, stress and mechanical quantities are nondimensionalized with respect to the shear modulus of the material, μ, and the volume fractions become unitless with respect to the maximum cellular volume fraction, ϕ_{max}. The nutrient concentration is

also scaled with respect to the concentration at the external boundary, c_b.

$$\tilde{R} = \frac{R}{R_{out}}, \quad \tilde{r} = \tilde{\chi} = \frac{\chi}{R_{out}}, \quad \widetilde{\Psi_p} = \frac{\Psi p}{R_{out}},$$

$$\tilde{t} = \frac{t}{t_r}, \quad \widetilde{\phi_s} = \frac{\phi_s}{\phi_{max}}, \quad \widetilde{c_n} = \frac{c_n}{c_b},$$

$$\widetilde{P_{appl}} = \frac{P_{appl}}{\mu\phi_{max}}, \quad (\widetilde{P_s^*})^{rR} = \frac{(P_s^*)^{rR}}{\mu\phi_{max}}, \quad (\widetilde{P_s^*})^{\vartheta\Theta} = \frac{(P_s^*)^{\vartheta\Theta}}{\mu\phi_{max}}$$

$$\tilde{\tau}(\widetilde{\phi_s}) = \frac{\tau(\phi_s)}{\mu\phi_{max}}, \quad \tilde{E} = \frac{E}{\mu},$$

$$\widetilde{k_p} = \frac{k_0\mu\phi_{max}t_r}{\nu R_{out}^2}, \quad \widetilde{D_n} = \frac{D_n t_r}{\phi_{max}R_{out}^2}, \quad \tilde{\zeta} = \zeta t_r, \quad \tilde{\lambda} = \frac{\lambda}{t_r}, \quad \widetilde{c_0} = \frac{c_0}{c_b}.$$

To simplify the notations, [15] drop the tildes and consider the parameters are all dimensionless. Then they discretize the dimensionless domain via Chebyshev nodes to solve the system numerically. A proper set of the nodes for polynomial interpolation can be obtained by dividing the interval $[R_{0,}1]$ into N+1 subintervals with varying width. This procedure allows them to convert a system of partial differential equations (Eqn. (18)-(21)) to the system of ordinary differential equations, which can be solved by an explicit Euler scheme.

2.1. Pure remodeling of a tumor spheroid with a necrotic core

Giverso and Preziosi [15] start by simulating pure remodeling after applying an external load on the outer boundary of a tumor spheroid whose necrotic core of radius R_0 is either composed of calcified debris or filled with water. The external load refers to the stress applied by a culture medium (e.g., gel) in vitro and by external tissues in vivo. Since cell growth takes longer than the application of the external load, they disregard growth in this case. Thus, the net production of the cellular phase is zero ($\Gamma_s = 0$) in (Eqn. (19)) and the

growth amplitude $g(t,R)=1$ for all t and R. To study the effect of remodeling in a MCTS in response to the external load, they consider four cases (Figure 3)

1) MCTS with a calcified core undergoing remodeling but not growth (Red line)

2) MCTS with a liquid core undergoing remodeling but not growth (Purple line)

3) MCTS with a liquid core undergoing neither remodeling nor growth (Light blue line)

4) MCTS with calcified core undergoing neither remodeling nor growth. (Blue line).

The authors simulate these cases by solving equations (Eqn. (18), (20), (23)) with initial conditions (Eqn. (24)-(25)), an external boundary condition (Eqn. (29)), and boundary conditions (Eqn. (30)-(31)) for either a calcified core or (Eqn. (33)-(34)) for a liquid core. They simulate two different remodeling scenarios by varying the remodeling threshold τ; they set τ to a small value (increasing the stress above the set threshold) to trigger remodeling and set τ to a larger value so that remodeling does not occur.

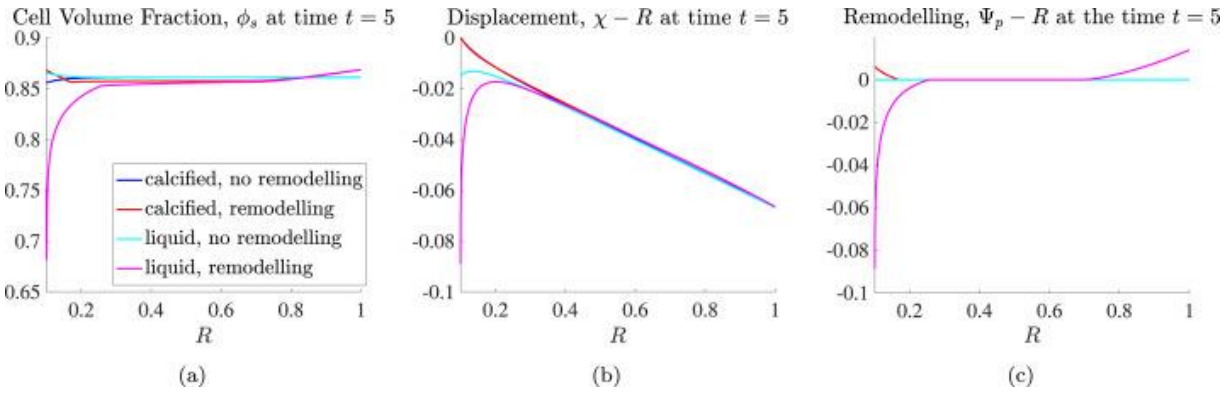

Figure 3. Influence of plastic reorganization in a tumor spheroid with either a calcified or a liquid core under an external load. At $t=5$, the MCTS with a rigid core and the one with a liquid cavity without remodeling are in steady states [1].

Figure 3 shows the values of the cell volumetric fraction $\phi_s(t,R)$, the displacement $\chi(t,R)-R$, and the plastic remodeling $\Psi_p(t,R)-R$ for a MCTS under external stress at

time $t = 5$. When first looking at the red line, which represents a spheroid with a calcified core undergoing remodeling, we can observe that the cell volumetric fraction increases at the outer boundary where stress is applied, and at the internal boundary where cells are pushed toward the calcified (rigid) core (Figure 3(a)). Since the change in volume of the solid phase, J, is inversely proportional to ϕ_s, J decreases as ϕ_s increases; thus the volume of the MCTS, the integral of J, decreases as well, implying negative displacements in Figure 3(b). Figure 3(b) also shows that the displacement of the spheroid with a calcified core undergoing remodeling (red line) is zero at the necrotic core due to Eqn. (30), but the spheroid has negative displacements on the other regions. Since the remodeling takes place near the inner and outer boundaries of the calcified spheroid (see red line on Figure 3(c)), the cell volumetric fraction near the necrotic core and the outer region is higher than that of the central region, where no plastic reorganization occurs. Moreover, remodeling occurs at the external boundary as soon as the stress is applied. If $\Psi_p - R < 0$, remodeling happens due to extensions along the R-axis and compression in the Θ and Φ directions. However, if $\Psi_p - R > 0$, remodeling takes place by compression along the radial direction and tension in the transverse directions.

When stress is applied to the outer boundary of the MCTS with a rigid necrotic core, the remodeling occurs at the external boundary due to compression along the R-axis and tension along the angular directions. Therefore, cells to pack more closely when the MCTS with a calcified core is constrained on both sides. Figure 3 implies that each layer of the aggregate (red line) has different mechanical behaviors; the central region of the aggregate has a visco-elastic behavior, whereas the region near the internal and external boundary has a visco-elasto-plastic behavior. In the central region, $\Psi_p - R = 0$, implying the elastic

behavior (Figure 3(c)). On the other hand, at the necrotic core and in the proliferative region, $\Psi_p - R > 0$, representing the occurrence of plastic remodeling. Therefore, the intersection of the core and the central region, and the intersection of the central region and the proliferative region have visco-elasto-plastic behaviors.

Next, we look at the case where a MCTS with a liquid core undergoes pure remodeling (purple line on Figure 3). Similar to the previous case, the cell volumetric fraction increases at the outer boundary in response to the external load. However, the aggregate has a smaller cell volumetric fraction near the internal boundary due to the absence of the rigid wall. Furthermore, the radius of the liquid core decreases, and the spheroid has negative displacements due to cell movement toward the core while water inside the core is flowing outward through the MCTS (Figure 3(b)). Similar to the tumor spheroid with a rigid calcified core undergoing remodeling (red line), the aggregate with a liquid core (purple line) experiences remodeling at both the internal and the external boundary. However, remodeling near the internal boundary occurs through extension along the radial direction, whereas remodeling near the external boundary occurs through the compression along the R-axis and the extension along the transverse direction.

Then, we look at the case in which a MCTS with a liquid cavity is under external load but does not experience remodeling due to a large value of τ (light blue line). Its cell volumetric fraction is almost constant, except for the slight increase in the compressed necrotic core, where the displacement is smaller. Since the blue and light blue lines do not experience remodeling, they have the same mechanical behavior in all MCTS layers, leading to smoother curves on Figure 3.

From Figure 3, we can see how remodeling and a composition of a necrotic core

influence the cell volumetric fraction and displacements of a spheroid. It is easier to observe the effects if a spheroid has a larger necrotic core (Figure 4). A MCTS not experiencing remodeling has the constant cell volumetric fraction regardless of its core component (Figure 4(a)). However, if remodeling occurs, a MCTS with a liquid core has decreasing φ^s at the necrotic core and increasing ϕ_s near the outer boundary, whereas a MCTS with a rigid core has increasing ϕ_s on both the inner and the outer boundaries. Moreover, the spheroid with the liquid necrotic core allows larger displacements at the inner and the external boundaries, compared to the one that does not experience remodeling (Figure 4(b)) A spheroid with a liquid core has larger displacements than the one with a calcified core, regardless of the occurrence of remodeling. Furthermore, if remodeling takes place, a spheroid with a liquid cavity has negative $\Psi_p - R$ at the necrotic core, whereas a spheroid with a calcified core has positive $\Psi_p - R$ at its core.

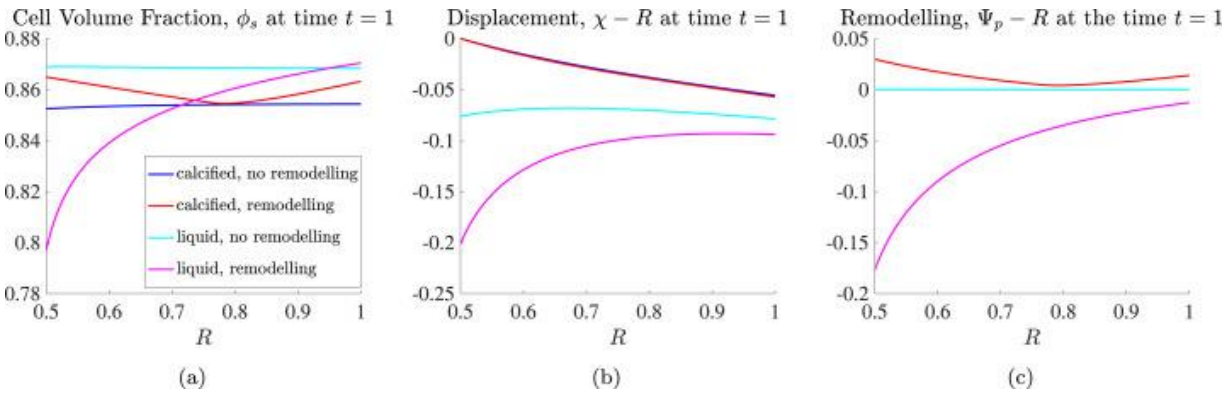

Figure 4. Influence of plastic reorganization on a tumor spheroid with either a calcified or a liquid core under an external load at time $t = 1$. The radius of the necrotic core R_0 is set to 0.5 [1].

2.2. Growth and remodeling of a tumor spheroid with a necrotic core

Next, we review the behavior of solutions when both cell growth and the external load on the outer boundary of a spheroid are considered by solving equations (Eqn. (18)-(21),

(23)) with the initial conditions (Eqn. (24)-(27)), external boundary conditions (Eqn. (28),(29)), and either (Eqn. (30)- (32)) for the calcified core or (Eqn. (33)-(35)) for the liquid core.

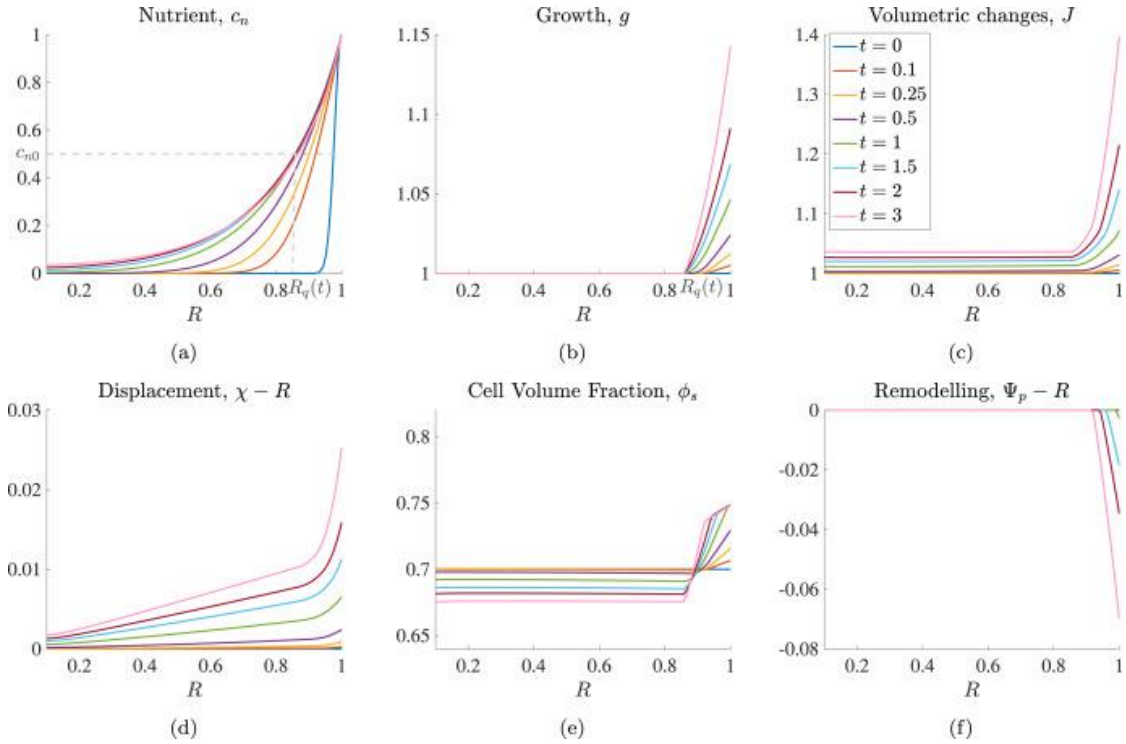

Figure 5. A spheroid with a liquid cavity undergoing free growth. The evolution of the different quantities over the radial coordinate for different times. The dimensionless parameters ($k_p = 0.7745, m_0 = 0.0848, m_1 = 4.638, \tau = 0.028, \lambda = 0.028, E = 0.28, c_{n0} = 0.5, D_n = 0.01$, and $\zeta = 0.5$) are used in this simulation [1].

We first show simulations of a MCTS with a liquid core expanding freely without an external load ($P_{appl} = 0$). Cells proliferate near the external boundary of the aggregate because sufficient nutrients are available from the microenvironment (Figure 5(a)). The quiescent region is defined as the region where the concentration of the nutrients (c_n) is not high enough to reach the set threshold for proliferation (c_{n0}), but above the level for necrosis. The radius of the quiescence region R_q depends on time and is controlled by the nutrient diffusive length and the MCTS expansion ($R_0 < R \leq R_q(t)$). The proliferative region is the

outer region of the MCTS where $R > R_q(t)$, and growth amplitude g is greater than 1 on that region, whereas g is equal to 1 in the quiescent region (Figure 5(b)). Figure 5(c) shows that volumetric changes, J, are greater than 1 in the entire region because of the tumor mass growth and are largest in the proliferative region. It is also clear from the positive displacement that the volume of the whole aggregate is increasing (Figure 5(d)). Since the increase in size of the quiescent region is not influenced by cell growth, the cell volumetric fraction of the region decreases as time progresses, whereas the cell volumetric fraction in the proliferative layer rapidly increases in time. The smaller cell volumetric fraction in the quiescence region compared to that in the proliferative region is consistent with the biological observations [23], which show that the quiescent region contains a larger amount of cytoplasmatic liquid than the proliferative region, where cells are more closely packed. It is evident from Figure 5(f) that remodeling occurs only near the outer boundary of the MCTS due to the structural reorganization by cell proliferation. It is also clear from Figure 5(e) that the proliferative domain can be divided into two subregions based on its capability of remodeling; the inner portion of the proliferative rim undergoes anelastic deformations by pure growth because the proliferation stress is below the remodeling threshold, whereas the outer portion experiences both growth and remodeling. However, this biphasic behavior depends on the chosen value of the remodeling threshold. The entire proliferative region of a MCTS can undergo remodeling for a small value of the threshold, and its cell volumetric fraction graph can be smoother. Remodeling affects the cell volume fraction, the stresses, the displacements, the volumetric changes of a MCTS, but the mechanical properties of the necrotic core scarcely influence the behavior of a growing MCTS (Figure 6).

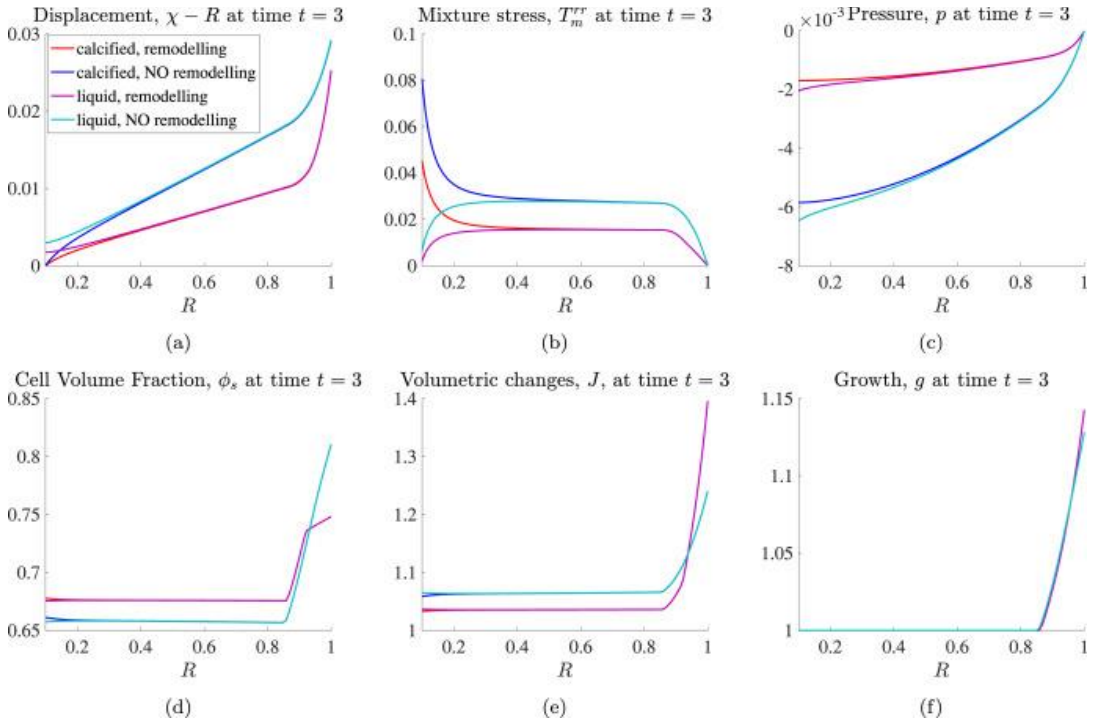

Figure 6. Influence of remodeling and free growth on a tumor spheroid with either a liquid or a calcified core at time $t = 3$ [1].

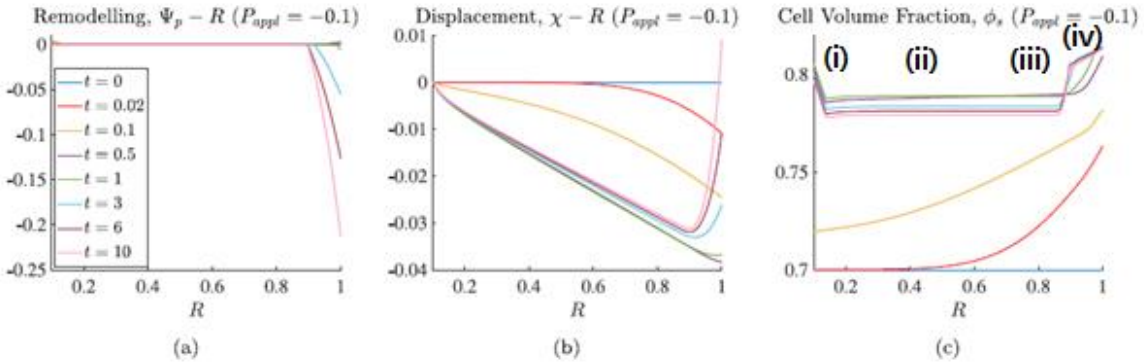

Figure 7. A spheroid with a calcified core growing under an external load. The parameters used in the simulation in Figure 5, except for $P_{appl} = -0.1$ and the remodeling threshold $\tau = 0.028$, are utilized here [1].

Finally, [15] study the behavior of growing MCTS under an applied stress, mimicking the stress applied by a gel or an external tissue. Figure 7(a) shows that remodeling occurs close to the internal and outer boundaries of the MCTS with a calcified core. At early times, $\Psi_p - R$ is positive on both boundaries due to the compression along the R-axis. However, as proliferation increases, remodeling keeps occurring at the internal boundary due to the cell

compression toward the rigid wall, and at the external boundary due to the extension along the R-axis by growth ($\Psi_p - R < 0$) (Figure 7(a) and (b)). Furthermore, looking at the final time points of Figure 7, we can observe that, for the particular value of the remodeling threshold and the external load used, remodeling only occurs in some portions of proliferative region. Thus, the entire MCTS can be divided into four subregions that have different mechanical behaviors: (i) the quiescent visco-elasto-plastic layer, (ii) the quiescent visco-elastic layer, (iii) the proliferative visco-elastic layer and (iv) the proliferative visco-elasto-plastic rim. However, with a higher applied load, a spheroid with a rigid core growing under an external load experiences remodeling in the entire proliferative region (Figure 8(a)), and the distribution of cell volume fraction becomes smoother than Figure 7(c) (Figure 8(c)).

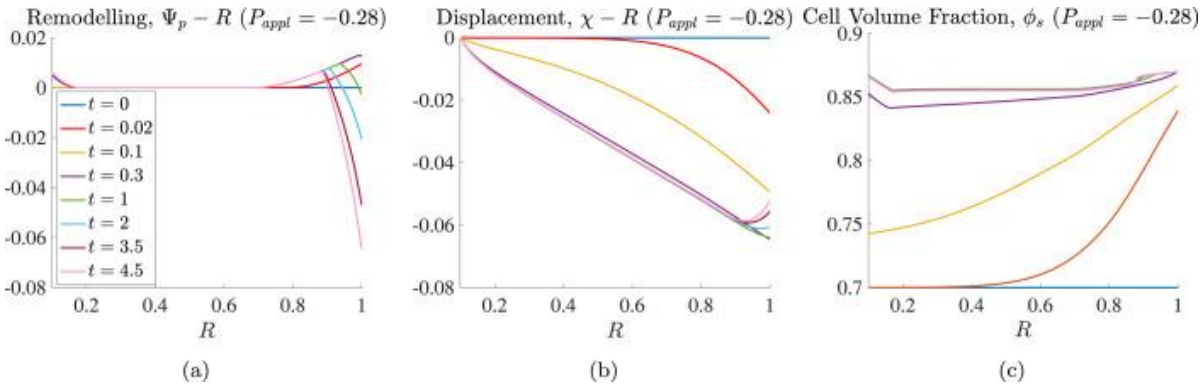

Figure 8. A spheroid with a calcified core growing under an external load ($P_{appl} = -0.28$). The parameters used in the simulation in Figure 7, except for the remodeling threshold $\tau = 0.028$, are utilized here [1].

2.3. Review

In [1], Giverso and Preziosi investigate the role of mechanical properties of the necrotic core on growth and remodeling of a tumor spheroid. In section 2.1, they study

remodeling of a spheroid with a necrotic core, composed of either a calcified debris or water, under an external load. The authors use two different values of τ to simulate the occurrence and the absence of remodeling in a tumor spheroid, and observe the evolution of cell volumetric fraction, displacement, and remodeling over the radial coordinate. From this simulation, Giverso and Preziosi observe that the tumor spheroid under an external load has varying mechanical behaviors based on the components of its necrotic core. In section 2.2, Giverso et al. investigate growth and remodeling of a tumor spheroid with a necrotic core. For a MCTS experiencing pure growth, remodeling triggered by setting a small remodeling threshold τ value can influence the behavior of the spheroid, regardless of its necrotic core constituent. In this case, the mechanical characteristics of the core component do not make significant changes on the response of a growing MCTS. For certain values of yield stress and applied load, a tumor spheroid growing under an external load can experience remodeling at the calcified core and a portion of its proliferative region, and the entire MCTS can be divided into subregions which have different mechanical behaviors. However, remodeling can take place in the entire proliferative region by setting a higher external load.

In my opinion, the result of [1] is worthy of notice because only a few studies have investigated the influence of the mechanical properties of the necrotic core on tumor progression. Giverso and Preziosi use a multiphase framework to introduce different mechanical properties of a necrotic core, either a calcified or a liquid core, and the influence of remodeling on the behavior of a MCTS. For this study, the authors clearly introduce a system of ordinary differential equations with the initial and boundary conditions, and they explicitly explain the meaning of each condition. Some figures presented in [1], but not all,

are well supported by biological experiments [23, 37-39], and most of the figures support the conclusions that they made. However, there are some issues that should be improved.

When describing the boundary conditions for their system, the descriptions and the conditions are somewhat mixed up (p. 24), and this may cause confusion to readers when understanding the model. For example, for the inner boundary of a spheroid with a calcified core, they state that there is no flux at the inner boundary and then that the inner boundary is fixed. However, when introducing the equations associated with these conditions, they present $\chi(t, R_0) = R_0$ first, and then $\Pi^R(t, R_0) = 0$, which are written in opposite order. To make it clearer, it would be better if the boundary descriptions are presented in the same order as the boundary equations.

For a spheroid experiencing free growth, Giverso and Preziosi [15] claim that the mechanical properties of the core's constituent do not make a significant difference on the behavior of the MCTS, excluding on the region close to the necrotic core (Figure 6). Based on this result, [15] assumes that this claim also applies to a MCTS with a necrotic core growing under an external load. However, they only present simulations of a spheroid with a calcified core growing under an external stress. Therefore, from only the figures that they present in [1], we cannot conclude that mechanical properties of a liquid necrotic core do not play critical role on tumor behavior when an external load is applied to the outer boundary of a growing spheroid. Supporting evidence for their claim and in particular a simulation of the growth of a spheroid with a liquid core under external stress is missing in [1].

Moreover, for the simulation of free growth of a MCTS with a necrotic core (Figure 6), Giverso and Preziosi say that "when no remodeling is triggered, the MCTS experiences lower displacements (Figure 6(a)), which are compensated by a higher ϕ_s (and consequently less

liquid) in the quiescent region with respect to the case in which remodeling does not occur (Figure 6(e))" (p. 29). When looking at the Figure 6(a) and (d), we observe that the MCTS remodeling actually has smaller displacements and a larger volumetric fraction, regardless of its core's composition. Thus, Giverso and Preziosi may have made a mistake when writing this assertion, which does not agree with the figures, and causes confusion to the readers.

In addition, Giverso and Preziosi made another minor mistake on their figure description. On the caption of Figure 3 in their paper, which is not shown in this thesis, they wrote MCTS as "MSCT". In addition, definitions of some mathematical variables, such as L_p, η, and γ_s, which are used in their model, are not given. Furthermore, the authors mention that an inner boundary of a growing MCTS with a liquid core "slightly penetrates the cavity" (p. 28) in the beginning of the simulation without showing any evidence. They assert this again in the conclusion. However, the authors should present supporting figures for this to be convincing.

In their studies of remodeling of a MCTS with either a calcified or a liquid core under an external load (Figure 3), time is set to t to 5, at which the spheroid with the calcified core (both with and without remodeling) and the one with the liquid core without remodeling reach steady state. In a separate simulation investigating a MCTS with a liquid core under an external load, they set time $t = 3$, at which the stationary condition is not yet reached, and do not mention when it reaches the steady state. Since some of their simulations do not reach steady state, the authors need to simulate the model for a longer time period to reach the stationary conditions for all simulations. Another issue with [15] is that cell death, either by necrosis or apoptosis, is not considered. At long times, these effects need to be considered.

Finally, Giverso and Preziosi assume that the MCTS grows symmetrically and does not develop irregular shapes. However, since tumors may undergo morphological instabilities and the host tissue is heterogeneous, tumors may not preserve their original shapes over time [22, 40-49]. Therefore, to study the behavior of aggressive and infiltrating tumors, further work needs to be done to study tumors with complex shapes. Furthermore, during necrosis, necrotic cells secrete molecules which may promote cancer progression through tissue inflammation [50]. And, beyond the mechanical forces induced by the microenvironment, it is well known that interactions between tumor and stromal cells can also significantly modify tumor behaviors [2]. This should also be investigated in future studies.

CHAPTER 3:

Survey of "An avascular tumor growth model based on porous media mechanics and evolving natural states" by Mascheroni et al.

Using mathematical modeling, Mascheroni et al. [2] investigate how the mechanical properties of the host microenvironment influence tumor growth, and the development of plastic and elastic deformations. Specifically, [2] investigates tumor growth in three different environments: a porous medium, in a soft host tissue and in a three-dimensional heterogeneous region. They investigate the influence of mechanical stress on cell behaviors, such as cell reorganization and proliferation.

Similar to Giverso and Preziosi [1], Mascheroni et al. [2] use a biphasic model for tumor development treating the tumor and microenvironment as porous media composed of solid and liquid phases and apply the theory of evolving natural configurations in their mathematical models. The solid phase represents the cancer cells and extracellular matrix (ECM), whereas the fluid phase is the interstitial fluid, which transports nutrients from the microenvironment to the tumor and thus supports tumor growth. In this paper, Maschernoni et al. [2] hypothesize that the solid phase (s) contains two types of cells, (i) proliferating cells (p) and (ii) necrotic cells (n), and a fluid phase (f) is composed of a nutrient (N) and another liquid component "water" (W), neglecting other biochemical components. The authors further do not distinguish between cells and ECM. They also assume that in vivo, the growing tumor is surrounded by either a soft host tissue, stiff host tissue (e.g. bone), or both. Thus, the region of space occupied by the system at time t (K_t) is divided into three disjoint subregions—the tumor tissue (T_t), a soft host tissue (H_t), and a stiff host tissue (B_t), and K_t can be written as $K_t = T_t \cup H_t \cup B_t$.

Similar to Giverso et al. in [1], Mascheroni et al. [2] use a biphasic, continuum biomechanical model along with advection-diffusion-reaction equations to describe nutrient transport. They set the saturation condition in T_t to be 1,

$$\phi_s + \phi_f = 1, \tag{36}$$

and they write the mass balance laws for the solid and the liquid phases and for the nutrient as [2]

$$\partial_t(\phi_s\, \rho^s) + (\phi_s\, \rho^s v^s) = \Gamma^s, \tag{37}$$

$$\partial_t\left(\phi_f\, \rho^f\right) + \left(\phi_f\, \rho^f v^f\right) = \Gamma^f, \tag{38}$$

$$\partial_t\left(\phi_f\, \rho^f \omega^N\right) + \left(\phi_f\, \rho^f \omega^N v^f\right) + \mathrm{Div}\, J^N = \Gamma^N_{N\to p}, \tag{39}$$

where ρ^α and v^α refer to the mass density and the velocity of the αth phase, respectively, and ω^N is the nutrient mass fraction. Γ^s (or Γ^f) denotes the mass exchange rate of the solid (or fluid) phase with the fluid (or solid) phase, and can be rewritten as $\Gamma^s = \Gamma^p_{p\to n} + \Gamma^p_{f\to p} + \Gamma^n_{p\to n} + \Gamma^n_{n\to f}$. $\Gamma^p_{p\to n}$ is defined as the rate at which proliferating cells turns into necrotic cells, and $\Gamma^p_{f\to p}$ describes the rate of increase of the proliferating cells based on mass exchange with the fluid phase. Moreover, $\Gamma^n_{p\to n}$ is the rate of necrosis, and $\Gamma^n_{n\to f}$ represents the rate of the necrotic cell dissolution. Therefore, since $\Gamma^p_{p\to n} + \Gamma^n_{p\to n} = 0$, Γ^s reduces to

$$\Gamma^s = \Gamma^p_{f\to p} + \Gamma^n_{n\to f}. \tag{40}$$

Because Mascheroni et al. [2] assume that the mass of their biphasic model is conserved, $\Gamma^s + \Gamma^f = 0$. They also assume momentum conservation:

$$\mathrm{Div}\,(\sigma^s + \sigma^f) = 0, \tag{41}$$

with the closure condition with respect to the momentum exchange rate (m), $m^s + m^f = 0$. σ^s and σ^f are the stress tensors of the solid and the liquid phases, respectively.

Similarly, in the host tissues H_t and B_t, the saturation condition is

$$\phi_s + \phi_f = 1, \quad \text{in } H_t \cup B_t. \tag{42}$$

Since the cells in the host do not proliferate and/or die, the mass balance laws for the solid and the fluid phases and for the nutrient in the subregions become

$$\partial_t(\phi_s \rho^s) + (\phi_s \rho^s v^s) = 0 \quad \text{in } H_t \cup B_t, \tag{43}$$

$$\partial_t(\phi_f \rho^f) + (\phi_f \rho^f v^f) = 0 \quad \text{in } H_t \cup B_t, \tag{44}$$

$$\partial_t(\phi_f \rho^f \omega^N) + (\phi_f \rho^f \omega^N v^f) + \text{Div } J^N = 0 \quad \text{in } H_t \cup B_t, \tag{45}$$

respectively. Indeed, the momentum balance laws of the system as a whole, considering the closure condition, $m^s + m^f = 0$, are

$$\text{Div } (\sigma^s + \sigma^f) = 0 \quad \text{in } H_t \cup B_t, \tag{46}$$

$$\text{Div } \sigma^f + m^f = 0 \quad \text{in } H_t \cup B_t. \tag{47}$$

If the fluid phase is considered as "macroscopically inviscid" and the components are supposed to be incompressible, the stress tensors σ^s and σ^f can be defined as [31, 51]

$$\sigma^s = \phi_s p^f I + \sigma^s_{eff} \quad \text{in } T_t \cup H_t \cup B_t, \tag{48}$$

$$\sigma^f = -\phi_f p^f I \quad \text{in } T_t \cup H_t \cup B_t. \tag{49}$$

I denotes the identity tensor, and p^f is the fluid pressure. σ^s_{eff} is the effective Cauchy stress tensor of the solid phase. This tensor is used to substitute for the Cauchy stress tensor to develop constitutive equations of elasticity and plasticity [52].

Eqn. (36)-(41) and (42)-(47) should be solved with the following conditions for the internal boundaries, which separate the three subdomains—T_t, H_t, and B_t:

$$\nu^s|_{I^{\alpha\beta}} \cdot n = \nu^s|_{I^{\beta\alpha}} \cdot n, \tag{50}$$

$$\phi_f \rho^f \nu^f|_{I^{\alpha\beta}} \cdot n = \phi_f \rho^f \nu^f|_{I^{\beta\alpha}} \cdot n, \tag{51}$$

$$(\phi_s \rho^f \omega^N \nu^f + J^N)|_{I^{\alpha\beta}} \cdot n = (\phi_s \rho^f \omega^N \nu^f + J^N)|_{I^{\beta\alpha}} \cdot n, \tag{52}$$

$$(\sigma^s + \sigma^f)|_{I^{\alpha\beta}}\, n = (\sigma^s + \sigma^f)|_{I^{\beta\alpha}}\, n, \tag{53}$$

$$\omega^N|_{I^{\alpha\beta}} = \omega^N|_{I^{\beta\alpha}}, \tag{54}$$

$$p^f|_{I^{\alpha\beta}} = p^f|_{I^{\beta\alpha}}. \tag{55}$$

$I^{\alpha\beta}$ represents the boundary between the αth and βth subregion, and the vertical bar $|_{I^{\alpha\beta}}$ (or $|_{I^{\beta\alpha}}$) indicates that this boundary is approached from the αth (or βth) side, where $\alpha, \beta = T_t$, H_t, and B_t.

In both the tumor and host soft tissues, the multiplicative decomposition of the deformation gradient tensor (Eqn. (1)) is used. To study the mechanical behavior of the system introduced in this work, [2] consider an undeformed (reference) configuration of the whole system, K_0 : $K_0 = T_0 \cup H_0 \cup B_0$, where T_0, H_0 , and B_0 are undeformed configurations of the subdomains of the system. Due to the existence of the disjoint subregions, the second Piola-Kirchhoff stress tensor relative to the reference configuration, S^i_{eff} is [2]

$$S^i_{eff} = \begin{cases} S^t_{eff} \text{ in } T_0, \\ S^h_{eff} \ in\ H_0, \\ S^b_{eff} \ in\ B_0. \end{cases} \tag{56}$$

where the Piola transformation $S^i_{eff} = J_a F_a^{-1} S^i_{v,eff} F_a^{-T}$ is used for $i = t, h, b$. Due to the isochoric plastic distortions, i.e., $J_p = 1$, the effective stress tensor for the tumor tissue becomes

$$S^t_{eff} = 2g b^t_1 B_p + 2b^t_2 \frac{1}{g}\left[\mathrm{tr}(CB_p)B_p - B_p C b_p\right] + 2b^t_3 \frac{J^2}{g^3} C^{-1}, \tag{57}$$

where g is tumor growth rate and $B_p = F_p^{-1}F_p^{-T}$. C represents the right on tensor, which is a measurement of deformation that is independent of rigid body rotation. According to Voyiadjis et al. [53], this tensor represents "the change in the square of relative position vector in an undeformed body to that of a deformed one." b_j^i can be calculated from the effective Piola-Kirchhoff stress tensor of the solid phase. The Piola-Kirchhoff stress tensor of a soft host tissue can also be obtained by setting $g = 1$ on Eqn. (57), since there is no growth in the healthy tissue. The stress tensor of the stiff host tissue is

$$S_{eff}^b = 2\mu^b E + \lambda^b \mathrm{tr}(E)I. \tag{58}$$

The following is used to model the plastic reorganization:

$$\dot{B}_p = -\frac{2\lambda_p}{||\mathrm{dev}\left(\sigma_{eff}^s\right)||}\langle||\mathrm{dev}\left(\sigma_{eff}^s\right)|| - \sqrt{2/3}\sigma_y\rangle_+ B_p \mathrm{dev}\left(\Sigma_{eff}^s\right), \tag{59}$$

where $\mathrm{dev}(\cdot)$ refers to the deviatoric part of the tensor of a tumor or a soft host tissue. σ_{eff}^s denotes the effective Cauchy stress in the solid phase, and σ_y stands for the yield stress at which a plastic deformation begins to occur. The Macaulay bracket $<\cdot>_+$ indicates that $< f >_+ = f$ if f is positive, and $< f >_+ = 0$ otherwise. Σ_{eff}^s is the Mandel stress tensor in the solid phase, where $\Sigma_{eff}^s = F^T P_{eff}^s$.

To study relations for the mass exchange terms, we recall the following equation:

$$\Gamma^s = \Gamma_{p\to n}^p + \Gamma_{f\to p}^p + \Gamma_{p\to n}^n + \Gamma_{n\to f}^n = \Gamma_{f\to p}^p + \Gamma_{n\to f}^n.$$

$\Gamma_{f\to p}^p$ indicates tumor growth, whereas $\Gamma_{n\to f}^n$ represents lysis. The former term is defined as

$$\Gamma_{f\to p}^p = \gamma_{fp}^p \langle\frac{\omega^N - \omega_{cr}^N}{\omega_{env}^N - \omega_{cr}^N}\rangle_+ \left(1 - \frac{\delta_1\langle\bar{\sigma}_{eff}^s\rangle_+}{\langle\bar{\sigma}_{eff}^s\rangle_+ + \delta_2}\right)\frac{\phi_f}{\phi_{f0}}\omega^p\phi_s, \tag{60}$$

where the nonnegative coefficient γ_{fp}^p indicates the nutrient consumption and interstitial fluids that increase tumor volume through cell growth. ω_{cr}^N is a nutrient threshold below

which cells do not proliferate, and ω_{env}^{N} is the mass fraction of oxygen in the microenvironment. $\bar{\sigma}_{eff}^{s}$ represents the spherical part of the effective Cauchy stress tensor of a solid phase, that is $\bar{\sigma}_{eff}^{s} = -\mathrm{tr}\left(\sigma_{eff}^{s}\right)/3$, and δ_1 and δ_2 are positive constants that describe the action of mechanical stress on cell proliferation ($\delta_1 < 1$). ϕ_{f0} is defined as the initial volumetric fraction of the fluid phase. Mascheroni et al. also introduce an equation that accounts for cell death due to the dissolution of necrotic cells in the interstitial fluid:

$$\Gamma_{n\to f}^{n} = \gamma_{nf}^{n}\omega^{n}\phi_s. \tag{61}$$

γ_{nf}^{n} is the cell dissolution coefficient. Moreover, the authors use the equation,

$$\Gamma_{p\to n}^{p} = -\gamma_{pno}^{p}\left\langle 1 - \frac{\omega^{N}}{\omega_{cr}^{N}}\right\rangle_{+}\omega^{p}\phi_s, \tag{62}$$

to describe necrosis. Nutrient transport from the interstitial fluid to the proliferating cells can be modeled by

$$\Gamma_{N\to p}^{N} = -\gamma_{Np1}^{N}\frac{\omega^{N}}{\omega^{N}+\gamma_{Np2}^{N}}\omega^{p}\phi_s. \tag{63}$$

Here, γ_{Np1}^{N} and γ_{Np2}^{N} are the coefficients that control the nutrient consumption of the proliferation cells.

Summarizing, the governing equations are [2]:

$$\phi_s = \frac{g^{3}\phi_{sv}}{J}, \tag{64}$$

$$\frac{\dot{g}}{g} = \frac{1}{3}\frac{\Gamma^{s}}{\phi_s\,\rho^{s}}, \tag{65}$$

$$\dot{\omega^{p}} = \frac{J}{\rho^{s}\phi_{sv}\,g^{3}}\left(\Gamma_{p\to n}^{p} + \Gamma_{f\to p}^{p} - \omega^{p}\Gamma^{s}\right), \tag{66}$$

$$J\phi_f\,\rho\dot{\omega^{N}} + \rho Q\cdot\mathrm{Grad}\,\omega^{N} + \mathrm{Div}\,\Psi^{N} = J\left(\Gamma_{N\to p}^{N} + \omega^{N}\Gamma^{s}\right), \tag{67}$$

$$\mathrm{Div}\,Q + \dot{J} = 0, \tag{68}$$

$$\mathrm{Div}\left(P_{eff}^{s} - Jp^{f}F^{-T}\right) = 0, \tag{69}$$

$$\dot{B}_p = -\frac{2\lambda_p}{||\mathrm{dev}(\sigma_{eff}^{s})||}\langle||\mathrm{dev}(\sigma_{eff}^{s})|| - \sqrt{2/3}\sigma_y\rangle_+ B_p \mathrm{dev}(\Sigma_{eff}^{s}), \tag{70}$$

where Q is the Piola transformation of the Darcy velocity:

$$Q = JF^{-1}\phi_f(v^f - v^s) = -JF^{-1}kF^{-T}\mathrm{Grad}\, p^f, \tag{71}$$

and Ψ^N is Fick's mass flux,

$$\Psi^N = -J\phi_f\rho F^{-1}D^N F^{-1}\mathrm{Grad}\,\omega^N \tag{72}$$

k describes a tensor for nutrient diffusivity, and D^N is the tissue hydraulic conductivity tensor. The unknowns in (Eqns. (65)-(70)) are:

$$U = \{g, \omega^p, \omega^N, p^f, \chi^s, \boldsymbol{B}_p\}. \tag{73}$$

3. 1. Growth of a tumor spheroid in the culture medium

Mascheroni et al. [2] first study a spherical tumor grown in vitro. The initial radius of the MCTS is taken to be to $100\ \mu m$ and the initial solid volume fraction is 0.8. The system of equations (Eqn. (65)-(70)) is solved with initial conditions,

$$g = 1, \quad \omega^p = 1, \quad \omega^N = \omega_{env}^N, \quad p^f = 0, \quad B_p = I \qquad \text{in } T_0,$$

and no normal flux and no normal displacement boundary conditions. The mass fraction of oxygen in the external environment ω_{env}^N is fixed, whereas the interstitial fluid pressure is zero. The yield stress in the tumor tissue is estimated based on the work of Iordan et al. [54], and the parameter values presented in Table 1 are used for this simulation. Furthermore, the system is solved by using the software package Comsol Multiphysics (COMSOL AB, Sweden).

Table 1. Parameters used to simulate behaviors of a tumor spheroid growing in a culture medium [2]. The references listed correspond to those in [2].

Symbol	Parameter	Unit	Value	Reference
φ_v^s	Solid volume fraction in the natural state	$(-)$	8.0×10^{-1}	[30]
ρ	Density of the phases	kg/m^3	1.0×10^3	[46]
k	Tumor hydraulic conductivity	$m^2/(Pa \cdot s)$	4.875×10^{-13}	[48]
D^N	Nutrient diffusion coefficient	m^2/s	3.2×10^{-9}	[46]
ω_{cr}^N	Critical level of nutrient	$(-)$	2.0×10^{-6}	[43]
ω_{env}^N	Environmental level of nutrient	$(-)$	7.0×10^{-6}	[65, 66]
γ_{Np1}^N	Coefficient related to nutrient consumption	$kg/(m^3 \cdot s)$	3.0×10^{-4}	[67, 68]
γ_{Np2}^N	Coefficient related to nutrient consumption	$(-)$	1.48×10^{-7}	[67, 68]
γ_{fp}^p	Coefficient related to growth	$kg/(m^3 \cdot s)$	5.348×10^{-3}	[69]
γ_{pno}^p	Coefficient related to necrosis	$kg/(m^3 \cdot s)$	1.5×10^{-1}	[43]
γ_{nf}^n	Coefficient related to lysis	$kg/(m^3 \cdot s)$	1.15×10^{-2}	[43]
λ_p	Coefficient related to cell reorganization time	$1/(Pa \cdot s)$	8.334×10^{-7}	[45]
σ_y^t	Yield stress	Pa	1.0×10^1	[44]
λ^t	Lamé's first parameter for the tumor	Pa	1.333×10^4	[48]
μ^t	Shear modulus for the tumor	Pa	1.999×10^4	[48]
δ_1	Coefficient related to growth inhibition	$(-)$	7.138×10^{-1}	[43]
δ_2	Coefficient related to growth inhibition	Pa	1.541×10^3	[43]

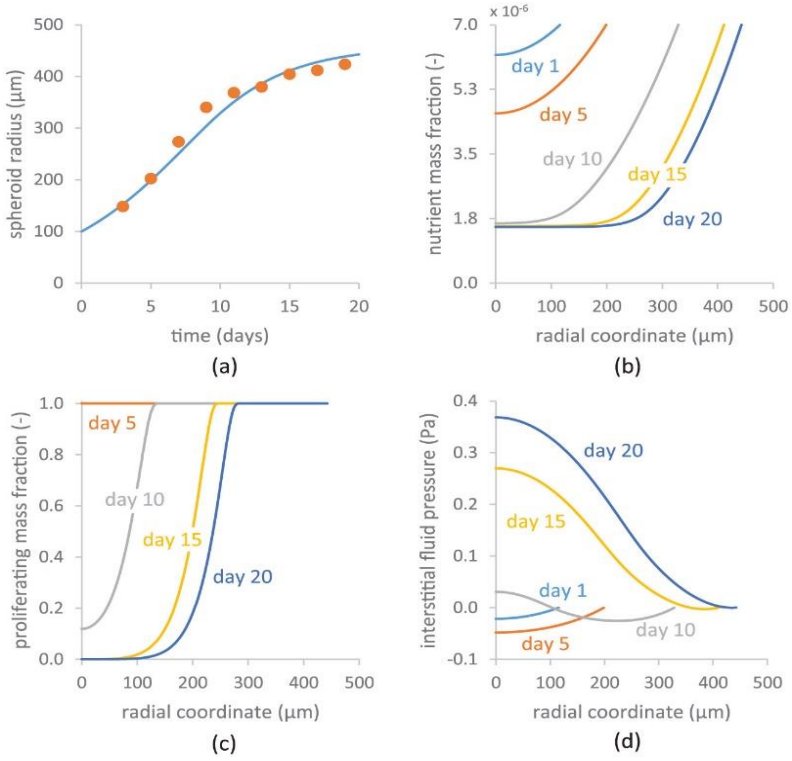

Figure 9. Behavior of a tumor spheroid growing in a culture medium. (a) Growth of a tumor spheroid is described with a solid line, whereas dots represent tumor growth based on experimental data from [55]. Evolution of (b) the nutrient mass fraction, (c) the mass fraction of proliferating cells, and (d) the interstitial fluid pressure over R-axis at the instant of time specified in the legend [2].

Figure 9(a) shows that the radius of the tumor spheroid increases as time goes by, and the result of the simulation (solid line) agrees with the biological experimental data (dots) from [55]. Figure 9(b) shows the evolution of the nutrient mass fraction inside the spheroid. Initially, the nutrients are distributed on the whole spheroid, but as time progresses, fewer nutrients are present in the center of the spheroid compared to its outer boundary. Due to the lack of nutrients in the center, the cells there die via necrosis, thus forming a necrotic core where the amount of nutrient supply is less than the threshold ω_{cr}^{N}. The existence of the core is also seen in Figure 9(c); a small fraction of proliferative cells resides in the center after day 10 of the simulation and no proliferative cells reside in the center after day 15, whereas all cells are proliferating at the outer region. Moreover, Figure 10(a) shows the growth stretch ratio g at different times, describing the tumor growth in the multiplicative decomposition of the deformation gradient. We can observe that g decreases in the center of a tumor spheroid because proliferating mass fraction is lower in the necrotic region than the outer proliferative region.

As seen in Figure 10(b), cell remodeling occurs throughout the entire MCTS as measured by the evolution of the trace of B_p. As the tumor grows, compressive stress appears at the boundary because tr $\left(\sigma_{eff}^{s}\right) < 0$, but the tissue located in the tumor interior experiences tension and tr $\left(\sigma_{eff}^{s}\right) > 0$ because of necrosis (Figure 10(c)). Furthermore, the von Mises stress is used to indicate the beginning of plastic flow (Eqn. (70) and Figure 10(d)). If the Von Mises stress is above the yield stress, then the material yields [56]. A nonzero value of the von Mises stress represents the occurrence of internal tissue reorganization, and its peak, which later slowly relaxes due to cell rearrangement, appears on the simulations after

day 10. The relaxation of the stress peak can be explained by the local increase in B_p (Figure 10(b)).

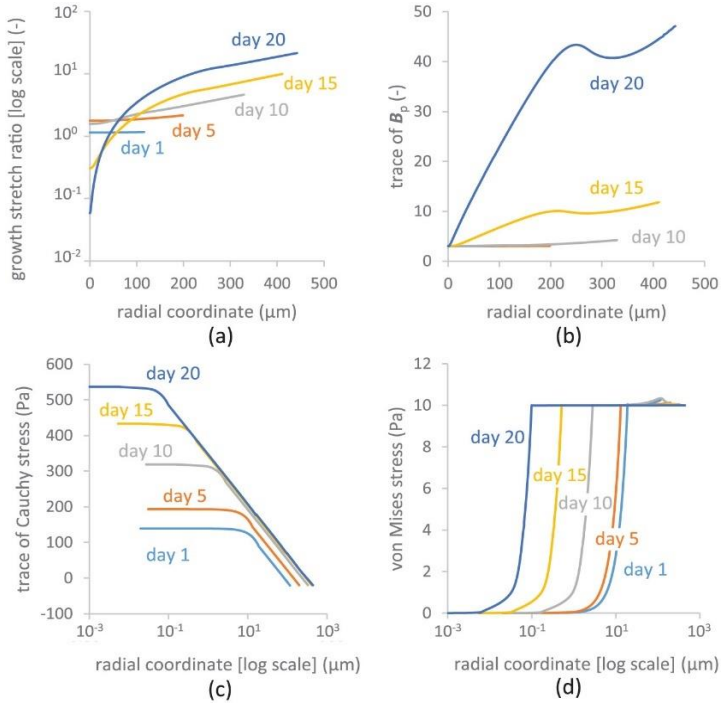

Figure 10. Evolution of different quantities over the radial coordinate at different times for a tumor spheroid growing in a culture medium [2].

The formation of the spheroid's necrotic core and the peak occur at the same time, and the peak in the von Mises stress and the boundary of the necrotic core are located at the same radial coordinate (Figure 11). This peak can be explained by the growth term Γ^s in Eqn. (65). Due to the lack of nutrients in the necrotic region, the $\Gamma^p_{f\to p}$ can be set to zero. Therefore, the time derivative of g,

$$\frac{\dot{g}}{g} = \frac{\Gamma^n_{n\to f}}{3\phi_s\rho} = -\frac{\gamma^n_{nf}\omega^n}{3\rho}, \tag{74}$$

becomes negative in the necrotic region, whereas the time derivative of g

$$\frac{\dot{g}}{g} = \frac{\Gamma^p_{f\to g}}{3\phi_s\rho} = -\frac{\gamma^p_{fp}}{3\rho}\left\langle\frac{\omega^N-\omega^N_{cr}}{\omega^N_{env}-\omega^N_{cr}}\right\rangle_+\left(1-\frac{\delta_1\langle\bar{\sigma}^s_{eff}\rangle_+}{\langle\bar{\sigma}^s_{eff}\rangle_+ +\delta_2}\right)\frac{\phi_f}{\phi_{f0}}\omega^p, \qquad (75)$$

is positive in the proliferative region. In other words, the value of g at its center at later times decreases due to a tumor volume reduction by necrosis, whereas the value of g increases at the outer boundary where cells proliferate due to sufficient nutrient supply.

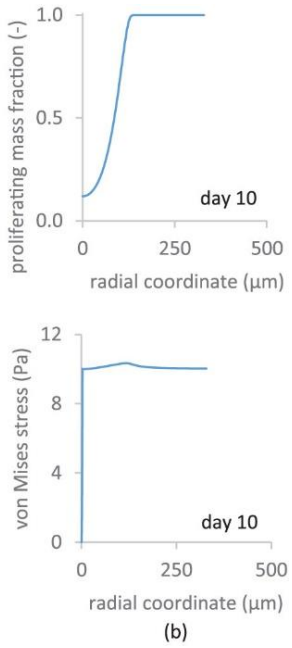

Figure 11. The mass fraction of proliferating cells and von Mises stress in a tumor spheroid on day 10 from the beginning of the simulation [2].

3. 2. Growth of a tumor in a soft host tissue

Next, Mascheroni et al. [2] investigates the influence of plastic reorganization in the soft host tissue. The system of equations (Eqn. (65)-(70)) coupled with the internal (Eqns. (50)-(55)) and the external boundary conditions is solved by COMSOL. The initial conditions are

$$g = 1, \quad \omega^p = 1 \text{in } T_0,$$

$$\omega^N = \omega^N_{env}, \quad p^f = 0, \quad B_p = I \ \text{ in } \ T_0 \cup H_0.$$

The fluid pressure, normal fluxes, and normal displacements are set to be zero, and ω^N_{env} is fixed. To account for the enhanced stability of cellular bonds in a tumor grown in a host tissue compared to one grown in vitro, longer times are required for cell reorganization, and the yield stress for the soft tissue should be higher. The parameters used in this situation are given is Table 2 and the results are shown in Figure 12.

Table 2. Parameters used to simulate behaviors of a tumor growing in a soft tissue [2]. The references listed correspond to those in [2].

Symbol	Parameter	Unit	Value	Reference
λ^h	Lamé's first parameter for the soft host tissue	Pa	3.336×10^3	[70]
μ^h	Shear modulus for the soft host tissue	Pa	5.0×10^3	[70]
σ_y^h	Yield stress for the soft host tissue[a]	Pa	1.0×10^3	–
λ_p	Coefficient related to cell reorganization time	$1/(\text{Pa} \cdot \text{s})$	8.334×10^{-8}	–
γ_{fp}^p	Coefficient related to growth	$\text{kg}/(\text{m}^3 \cdot \text{s})$	8.022×10^{-3}	[71]
ω_{cr}^N	Critical level of nutrient	(−)	1.0×10^{-6}	–
ω_{env}^N	Environmental level of nutrient	(−)	4.2×10^{-6}	[46]

[a] Value assumed when plastic rearrangement in the soft host tissue is taken into account.

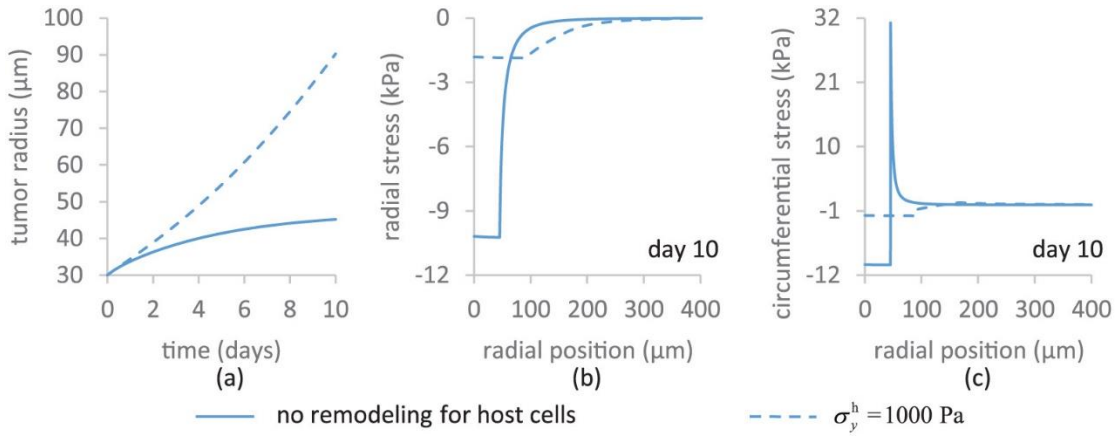

Figure 12. A tumor growing in a healthy tissue in which remodeling occurs (solid lines) or is neglected (dashed lines). Evolution of (a) the tumor radius over time, (b) radial stress, and (c) the circumferential stress for different times [2].

In Figure 12, the solid lines represent the case where the mechanical parameters of Table 2 are used and where no remodeling occurs in the host tissue; the dashed lines refer to the case in which a remodeling takes place in the host tissue. The latter case displays faster tumor growth than the former case (Figure 12(a)) because of the stress relaxation caused by remodeling. On day 10 of the simulation, the latter case (dashed line) has smaller magnitudes of radial and circumferential stresses and a smoother transition between the tumor and the host tissue (Figure 12(b) and (c)). Higher mechanical stress on the tumor boundary forms a stronger mechanical barrier. This may limit the tumor growth, thus resulting in the smaller tumor sizes and less host tissue displacement.

3. 3. Growth of a tumor in a heterogeneous environment

Finally, Mascheroni et al. studies a growing tumor surrounded by a microvessel, i.e. a blood capillary, and different adjacent tissues (Figure 13(a)). In this case, the system of equations (Eqn. (65)-(70)) is solved with initial conditions,

$$g = 1, \quad \omega^p = 1 \qquad \text{in } T_0,$$

$$B_p = I \qquad \text{in } T_0 \cup H_0,$$

$$\omega^N = \omega^N_{cap}, \quad p^f = 0 \qquad \text{in } K_t,$$

and boundary conditions, which are described in Figure 13(b). Here, ω^N_{cap} is the mass fraction of nutrients transported from the blood vessel, and it is fixed on the surfaces of the capillary. The value of the yield stress of the healthy tissue is fixed to $\sigma^h_y = 10^3$ Pa, and the other parameters are presented in Table 3. The parameters not shown in this table are given in Table 1 and 2.

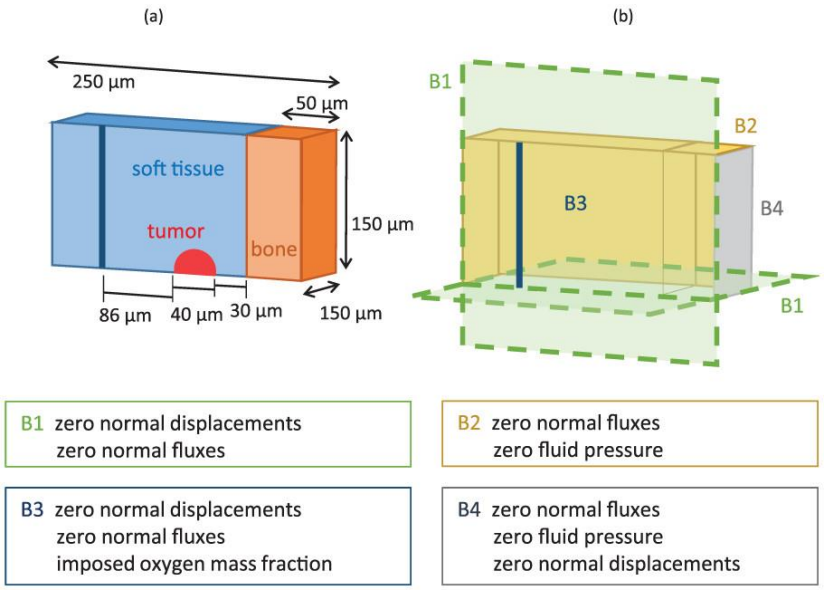

Figure 13. "Geometry of the problem and boundary conditions for a tumor" growing in a blood capillary and two different host tissues [2].

Table 3. Parameters used to simulate behaviors of a tumor growing in a heterogeneous environment [2]. The references listed correspond to those in [2].

Symbol	Parameter	Unit	Value	Reference
λ^{b}	Lamé's first parameter for the bone tissue	Pa	5.769×10^{9}	[72, 73]
μ^{b}	Shear modulus for the bone tissue	Pa	3.846×10^{9}	[72, 73]
φ^{b}	Bone porosity	(−)	6.0×10^{-1}	[72, 73]
k^{b}	Bone hydraulic conductivity	$m^2/(Pa \cdot s)$	3.0×10^{-15}	[72, 73]
R_0	Tumor initial diameter	μm	40	–
ω^{N}_{cap}	Capillary oxygen mass fraction	(−)	4.2×10^{-6}	[46]
ω^{N}_{cr}	Critical oxygen mass fraction	(−)	3.0×10^{-6}	–
γ^{p}_{fp}	Coefficient related to growth	$kg/(m^3 \cdot s)$	1.0×10^{-2}	–
λ_p	Coefficient related to cell reorganization time	$1/(Pa \cdot s)$	1.389×10^{-8}	–

Due to the varying mechanical environment, the tumor grows asymmetrically. On day 7 of the simulation, the tumor is less likely to grow in the direction of the bone tissue because of its larger stiffness, whereas the tumor is more likely to grow in the direction of the capillary surfaces. Larger values of total displacements are found on the tumor side of the capillary surfaces because of the higher nutrient supply (Figure 14(a), (c), and Figure 15). On the other hand, the total displacements are lower on the tumor side of the bone tissue,

which has lower nutrient mass fraction. Figure 14(c) also shows that the nutrients are reduced at the center of the tumor. Lastly, Figure 14(d) represents the trace of B_p on day 7, showing that remodeling occurs in tissues external to the tumor. This result confirms that the growth of the tumor leads to the displacement of the healthy tissue and the plastic rearrangement of the host cells.

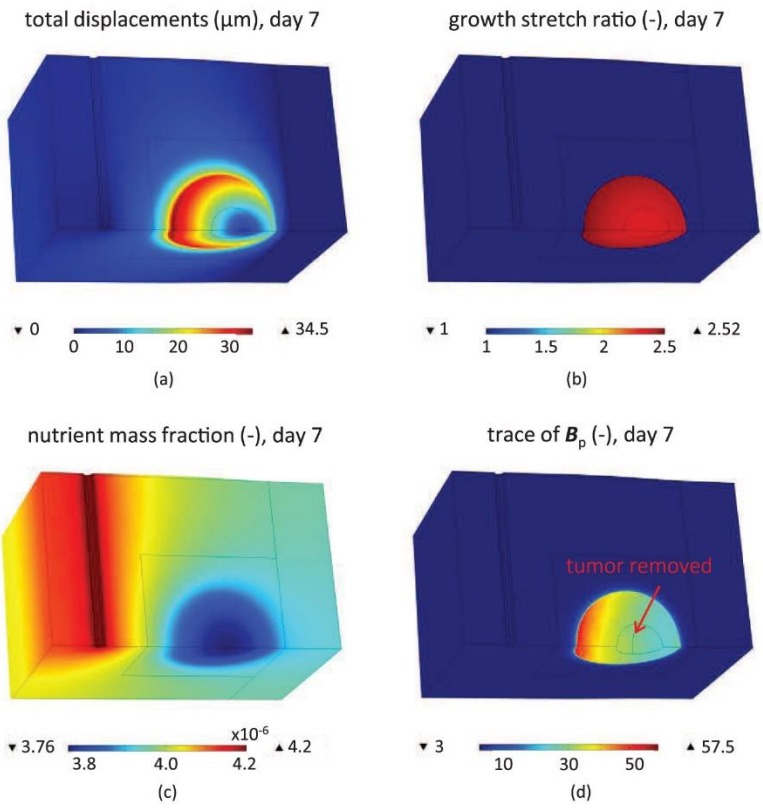

Figure 14. A tumor growing in a heterogeneous environment. The evolution of (a) the solid displacements, (b) the growth stretch ratio, (c) the nutrient mass fraction, and (d) the trace of B_p over the tissues external to the tumor on day 7, which is the end of the simulation [2].

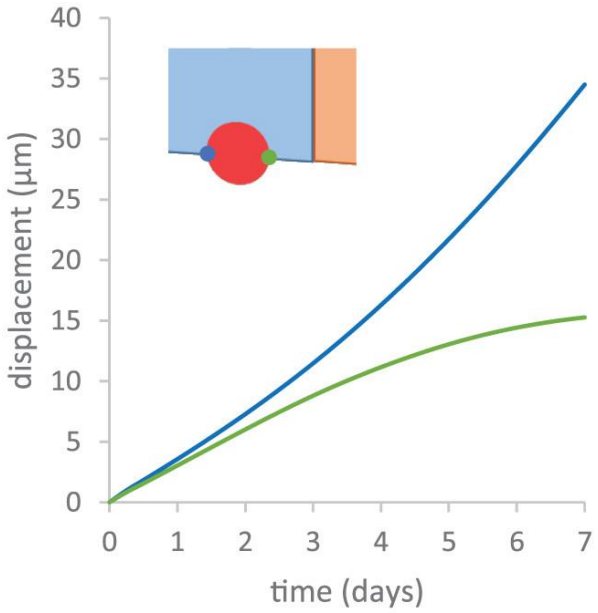

Figure 15. Displacements of a tumor growing in a heterogeneous environment are measured at two different locations [2].

3. 4. Review

In [2], Mascheroni et al. study a tumor growing in three different microenvironments, having different mechanical characteristics. First, they investigate the growth of a tumor spheroid in a culture medium. In Figure 9-11, the authors observe the formation of a necrotic region, in which nutrient is deficient, and a proliferative region, where sufficient nutrients are transported from an external environment. Next, to study the behavior of a tumor growing in a soft host tissue, Mascheroni et al. [2] simulate the evolution of the tumor radius, radial stress, and circumferential stress in two different cases, where plastic deformation in the soft host tissue is considered and neglected. Through the simulation, the authors observed that the tumor grows faster when its soft host tissue experiences remodeling. Lastly, the authors investigate the tumor development in a three-dimensional heterogeneous region. They observe that a tumor side closer to a blood vessel has a higher displacement and remodeling, compared to the one closer to a bone. Moreover, a soft tissue near the vessel

has the higher nutrient mass fraction.

In my opinion, the work of Mascheroni et al. [2] is worthy of notice because dependence of tumor development on the external microenvironment is more fully explored than in many previous studies. The work of Mascheroni et al. [2] shows that tumor development is closely related to the mechanical properties of a tumor microenvironment. They present the mass balance laws for tumors living in different environments and include cell death in the mass exchange terms Γ^s, whereas Giverso et al. [1] do not include cell death in their model. Further, Mascheroni et al. define all variables used in their mathematical model, and they clearly describe how they derived the final form of the equations of their model. Mostly, their assertions and conclusions are well supported by figures and results presented on the paper, and some of the results agree with biological experiments [8, 55]. Despite their effort and hard work, there are some issues that need to be improved.

To investigate impact of plastic remodeling of a soft host tissue on tumor growth, Mascheroni et al. [2] simulate the evolution in two different cases, where plastic deformation in the soft host tissue is considered and neglected. However, for a tumor growing in a heterogeneous environment, the authors only consider the case in which rearrangement of the host cells occurs but they did not explore the case in which plastic reorganization is neglected in the host tissues. Therefore, for a better understanding of the effects of tissue remodeling on tumor development, it would be better if they provide results for both cases so that readers can clearly see differences.

Moreover, compared to the growth of a tumor spheroid in vitro, in vivo tumor growth in heterogeneous environments (the tumor growth in the presence of a blood vessel and two different host tissues) has been less investigated by Mascheroni et al [2]. For example, the

distributions of the different types of stress—Cauchy, Von Mises, radial, and circumferential stress—over radial coordinate are not shown in their paper.

For a tumor growing near a microvessel and in different adjacent host tissues, Mascheroni et al. [2] claim that the tumor grows asymmetrically due to different chemomechanical properties of its microenvironment. In other words, a tumor side closer to a blood vessel has a higher displacement than the one closer to a stiff tissue, i.e. a bone, and the authors offer their readers Figure 15 as supporting evidence for their claim. The figure contains two curves—a green (stiff side) and a blue (soft side) curve, and they slowly diverge as time goes by. The divergence of the curves implies the different displacements of a tumor depending on the location that is measured. Even though Mascheroni et al. [2] provide a small inset that shows a specific area that each color represents, it is hard to see it if the readers do not look at it closely. Moreover, the authors did not mention anything about the color representation of the curves in their work. Therefore, it would be better if they offer their readers a proper description of each color on the figure in order to make the graph more understandable.

Mascheroni et al. [2] also made a typographical error when referring to Figure 3 in their paper (which is not presented in this thesis), which is referred as “Figure. 3.2” (p. 696). In addition to this, they use wrong reference number when referring the work of Iordan et al. [54]. The reference number for the work is “[45]”, whereas Mascheroni et al. referred it as “[44]” (p.696).

To study the role of mechanical stress on tumor growth and remodeling, a novel feature of the approach in [2] is the incorporation of two types of tumor cells and three different microenvironmental components. However, further investigations should be

performed to test their simplified model assumptions. For example, since ECM is not considered explicitly in this model, future studies need to include cell migration through the ECM [57] and different stiffness levels between cell-filled and cell-empty regions of the ECM. The authors should also study interactions—such as detachment or adhesion— between the cells and ECM. Additional work should also incorporate different adhesive characteristics of each cell type, which would lead to a modification of the yield stress expression in their models. Further experiments and new data sets are required to better approximate model parameters, such as the yield stress, and to validate and refine the models. Lastly, different mechanical characteristics of compressive stress and shear stress should be considered. By investigating biochemomechanical interactions between a tumor and its microenvironment, the variable growth patterns and tumor progression observed in experiments and in patients can be better understood.

CHAPTER 4: CONCLUSION

The studies of Giverso et al. [1] and Mascheroni et al. [2] both use mathematical models to investigate the effect of mechanical stress on cell behaviors. In particular, they simulate growth of a MCTS under external mechanical loads, which mimic stresses applied by a gel in in vitro cultures and by the host microenvironment in vivo. Mascheroni et al. [2], however, go on to model chemomechanical heterogeneities in the host tissue by considering soft tissue, hard tissue (e.g., bone) and the presence of a blood vessel.

Both papers present biphasic models of tumor growth where the tumor (and host tissue) are treated as a porous medium that is composed of a solid phase and a liquid phase, and these models are based on the concept of evolving natural configurations. And, in both cases, tumor growth is dependent on the presence of nutrients, which are transported through the interstitial liquid to, and throughout, the tumor.

Giverso et al. [1] assume that the solid phase is a mixture of different types of cell populations — necrotic cells, quiescent cells, and proliferative cells — and they divide a tumor spheroid into three layers: a necrotic core, a quiescent region, and a proliferative ring. Focusing on the mechanical properties of the necrotic core, Giverso et al. [1] study the behavior of a MCTS with different components in the core (either calcified debris or a liquid cavity), and do not take into account its external mechanical environment, other than the growth medium. They do not account for cell death inside a tumor in their model as well.

Giverso et al. [1] divide their study into three cases: the case where a MCTS is under stress without growth, where a MCTS experiences free growth, and where a growing MCTS is under an external load. In the first case, with a sufficiently large necrotic region, the MCTS shows different mechanical behaviors based on the constituent of its core. However, in the

second and third cases, the precise composition of the necrotic core is not important. Instead, the cell behaviors are mainly characterized by plastic reorganization that occurs inside the spheroid. Giverso et al. [1] also show that the growing MCTS under stress can be divided into four subregions, which have different mechanical properties (Figure 7). They claim that, with small external stress, only a portion of the proliferative region can experience plastic reorganization, and remodeling in the entire proliferative region can be achieved by increasing the external load (Figure 8). However, some of studies, such as that shown in Figure 3 (here) and Figure 6 (of their paper, not presented here), are not simulated for enough time, and thus stationary conditions were not reached and thus it is not clear how the forces balane in the long-term. Moreover, Giverso et al. [1] did not consider cell death in their model, which could significantly impact tumor dynamics.

On the other hand, Mascheroni et al. [2] assume that the solid phase is made up of proliferative cells and necrotic cells with the ECM, and that the tumor spheroid is embedded in a heterogeneous host microenvironment. Mascheroni et al. [2] investigate the effect of the mechanical environments around the tumor spheroid on its growth and remodeling, and the effect of relaxing the stress by plastic reorganization. In contrast to Giverso et al. [1] , Mascheroni et al. [2] did not divide the proliferative region into subregions, and thus they did not describe the different types of cell behaviors within the region. Interestingly, Mascheroni et al. [2] observe a peak in the von Mises stress when proliferative cells undergo necrosis, which drives remodeling and stress relaxation.

In the case where a tumor spheroid grows in a healthy tissue, Mascheroni et al. [2] consider the cases in which plastic reorganization is neglected or included in the tissue. Compared to the latter case, the former case has a smaller tumor radius, and larger

magnitudes of the radial and the circumferential stresses. Finally, when a tumor is grown in a heterogeneous host tissue, which is composed of a soft tissue and a stiff tissue, the tumor growth is characterized by the different mechanical characteristics of each tissue. Due to the different stiffness levels of the tissues, the tumor grows more in the softer tissue, which has less mechanical resistance. Also different from Giverso et al. [1], Mascheroni et al. [2] consider cell death in their model.

Both Giverso et al. [1] and Mascheroni et al. [2] assume symmetrical growth of a tumor spheroid in culture, and the latter goes on to study heterogeneous tumor growth induced by biochemomechanical heterogeneities in the microenvironment. However, the study presented was quite limited and much more work needs to be done to investigate the role of heterogeneities on tumor growth. Further, additional signaling between tumor cells and tumor and stromal cells, which may promote cancer progression and development, is neglected in both studies. Mascheroni et al. [2] and Giverso et al. [1] also fail to account for the existence of ECM and the relation between the ECM and the tumor. Therefore, future studies should investigate the influence of cell-ECM interactions, and cell-cell signaling, on cell behaviors. In addition, more and better curated experimental data sets are also required to improve mathematical models and to estimate parameter values. Lastly, improved mathematical models and careful simulation studies will provide much needed insight on tumor progression and should shed light on the development of new and improved strategies for treating tumors by improving the delivery and efficacy of chemotherapy, nanotherapeutics, and radiotherapy.

REFERENCE

1. Giverso, C. and L. Preziosi, *Influence of the mechanical properties of the necrotic core on the growth and remodelling of tumour spheroids.* International Journal of Non-Linear Mechanics, 2019. **108**: p. 20-32.
2. Mascheroni, P., et al., *An avascular tumor growth model based on porous media mechanics and evolving natural states.* Mathematics and Mechanics of Solids, 2018. **23**(4): p. 686-712.
3. Kalli, M. and T. Stylianopoulos, *Defining the Role of Solid Stress and Matrix Stiffness in Cancer Cell Proliferation and Metastasis.* Front Oncol, 2018. **8**: p. 55.
4. Jain, R.K., J.D. Martin, and T. Stylianopoulos, *The Role of Mechanical Forces in Tumor Growth and Therapy.* Annual Review of Biomedical Engineering, 2014. **16**(1): p. 321-346.
5. Cheng, G., et al., *Micro-environmental mechanical stress controls tumor spheroid size and morphology by suppressing proliferation and inducing apoptosis in cancer cells.* PloS one, 2009. **4**(2): p. e4632-e4632.
6. Desmaison, A., et al., *Mechanical Stress Impairs Mitosis Progression in Multi-Cellular Tumor Spheroids.* PLOS ONE, 2013. **8**(12): p. e80447.
7. Frank, V., et al., *Frequent mechanical stress suppresses proliferation of mesenchymal stem cells from human bone marrow without loss of multipotency.* Scientific Reports, 2016. **6**(1): p. 24264.
8. Helmlinger, G., et al., *Solid stress inhibits the growth of multicellular tumor spheroids.* Nat Biotechnol, 1997. **15**(8): p. 778-83.
9. Lee, D.A., et al., *Stem cell mechanobiology.* J Cell Biochem, 2011. **112**(1): p. 1-9.
10. Montel, F., et al., *Stress clamp experiments on multicellular tumor spheroids.* Phys Rev Lett, 2011. **107**(18): p. 188102.
11. Delarue, M., et al., *Compressive stress inhibits proliferation in tumor spheroids through a volume limitation.* Biophys J, 2014. **107**(8): p. 1821-1828.
12. Humphrey, J. and K. Rajagopal, *A constrained mixture model for growth and remodeling of soft tissues.* Mathematical Models and Methods in Applied Sciences, 2011. **12**.
13. Humphrey, J.D. and K.R. Rajagopal, *A constrained mixture model for arterial adaptations to a sustained step change in blood flow.* Biomech Model Mechanobiol, 2003. **2**(2): p. 109-26.
14. Rodriguez, E.K., A. Hoger, and A.D. McCulloch, *Stress-dependent finite growth in soft elastic tissues.* J Biomech, 1994. **27**(4): p. 455-67.
15. Skalak, R., et al., *Compatibility and the genesis of residual stress by volumetric growth.* Journal of Mathematical Biology, 1996. **34**(8): p. 889-914.
16. NDT Resources Center. *Elastic/plastic deformation*. Available from: https://www.nde-ed.org/EducationResources/CommunityCollege/Materials/Structure/deformation.htm.
17. Rajagopal, K.R. and A.R. Srinivasa, *On the thermomechanics of materials that have multiple natural configurations Part I: Viscoelasticity and classical plasticity.* Zeitschrift für angewandte Mathematik und Physik ZAMP, 2004. **55**(5): p. 861-893.
18. Průša, V. and K. Rajagopal, *On models for viscoelastic materials that are mechanically incompressible and thermally compressible or expansible and their Oberbeck--Boussinesq type approximations.* Mathematical Models and Methods in Applied Sciences, 2013. **23**.
19. Cui, X., Y. Hartanto, and H. Zhang, *Advances in multicellular spheroids formation.* Journal of the Royal Society, Interface, 2017. **14**(127): p. 20160877.
20. Wallace, D.I. and X. Guo, *Properties of tumor spheroid growth exhibited by simple mathematical models.* Frontiers in oncology, 2013. **3**: p. 51-51.
21. Chaplain, M.A.J., *Avascular growth, angiogenesis and vascular growth in solid tumours: The mathematical modelling of the stages of tumour development.* Mathematical and Computer Modelling, 1996. **23**(6): p. 47-87.
22. Folkman, J. and M. Hochberg, *Self-regulation of growth in three dimensions.* The Journal of experimental medicine, 1973. **138**(4): p. 745-753.
23. Sherar, M.D., M.B. Noss, and F.S. Foster, *Ultrasound backscatter microscopy images the internal structure of living tumour spheroids.* Nature, 1987. **330**(6147): p. 493-495.
24. Acland, M., et al., *Mass Spectrometry Analyses of Multicellular Tumor Spheroids.* PROTEOMICS - Clinical Applications, 2017. **12**: p. 1700124.

25. Groebe, K. and W. Mueller-Klieser, *Distributions of oxygen, nutrient, and metabolic waste concentrations in multicellular spheroids and their dependence on spheroid parameters.* European Biophysics Journal, 1991. **19**(4): p. 169-181.
26. Kerr, J.F.R., C.M. Winterford, and B.V. Harmon, *Apoptosis. Its significance in cancer and cancer Therapy.* Cancer, 1994. **73**(8): p. 2013-2026.
27. Krysko, D.V., et al., *Apoptosis and necrosis: detection, discrimination and phagocytosis.* Methods, 2008. **44**(3): p. 205-21.
28. Cheng, J.M., et al., *Malignant abdominal rocks: where do they come from?* Cancer Imaging, 2013. **13**(4): p. 527-39.
29. Coleman, J.F., *Robbins and Cotran's Pathologic Basis of Disease, 8th Edition.* The American Journal of Surgical Pathology, 2010. **34**(1): p. 132.
30. Grillo, A., et al., *Mass Transport in Porous Media With Variable Mass*, in *Numerical Analysis of Heat and Mass Transfer in Porous Media*, J.M.P.Q. Delgado, A.G.B. de Lima, and M.V. da Silva, Editors. 2012, Springer Berlin Heidelberg: Berlin, Heidelberg. p. 27-61.
31. Majid Hassanizadeh, S., *Derivation of basic equations of mass transport in porous media, Part 2. Generalized Darcy's and Fick's laws.* Advances in Water Resources, 1986. **9**(4): p. 207-222.
32. Giverso, C. and L. Preziosi, *Modelling the compression and reorganization of cell aggregates.* Mathematical medicine and biology : a journal of the IMA, 2011. **29**: p. 181-204.
33. Marciniak, Z., J.L. Duncan, and S.J. Hu, *2 - Sheet deformation processes*, in *Mechanics of Sheet Metal Forming (Second Edition)*, Z. Marciniak, J.L. Duncan, and S.J. Hu, Editors. 2002, Butterworth-Heinemann: Oxford. p. 14-29.
34. Ambrosi, D. and L. Preziosi, *Cell adhesion mechanisms and stress relaxation in the mechanics of tumours.* Biomechanics and Modeling in Mechanobiology, 2008. **8**(5): p. 397.
35. Grillo, A., S. Federico, and G. Wittum, *Growth, mass transfer, and remodeling in fiber-reinforced, multi-constituent materials.* International Journal of Non-linear Mechanics - INT J NON-LINEAR MECH, 2012. **47**.
36. ADEEB, S. *STRESS: FIRST AND SECOND PIOLA-KIRCHHOFF STRESS TENSORS*. [cited 2019 December 3]; Available from: https://sameradeeb-new.srv.ualberta.ca/stress/first-and-second-piola-kirchhoff-stress-tensors/.
37. Chandrasekaran, S. and M. King, *Gather Round: In vitro tumor spheroids as improved models of in vivo tumors.* J Bioengineer & Biomedical Sci, 2012. **2**.
38. Cui, X., Y. Hartanto, and H. Zhang, *Advances in multicellular spheroids formation.* J R Soc Interface, 2017. **14**(127).
39. Grimes, D.R., et al., *A method for estimating the oxygen consumption rate in multicellular tumour spheroids.* J R Soc Interface, 2014. **11**(92): p. 20131124.
40. Sutherland, R., *Cell and environment interactions in tumor microregions: the multicell spheroid model.* Science, 1988. **240**(4849): p. 177-184.
41. Sutherland, R.M. and R.E. Durand, *Growth and cellular characteristics of multicell spheroids.* Recent Results Cancer Res, 1984. **95**: p. 24-49.
42. Byrne, H. and P. Matthews, *Asymmetric growth of models of avascular solid tumours: exploiting symmetries.* IMA J Math Appl Med Biol, 2002. **19**(1): p. 1-29.
43. Byrne, H.M. and M.A.J. Chaplain, *Growth of nonnecrotic tumors in the presence and absence of inhibitors.* Mathematical Biosciences, 1995. **130**(2): p. 151-181.
44. Byrne, H.M. and M.A.J. Chaplain, *Growth of necrotic tumors in the presence and absence of inhibitors.* Mathematical Biosciences, 1996. **135**(2): p. 187-216.
45. Byrne, H.M. and M.A.J. Chaplain, *Free boundary value problems associated with the growth and development of multicellular spheroids.* European Journal of Applied Mathematics, 1997. **8**(6): p. 639-658.
46. Cross, S.S. and D.W. Cotton, *The fractal dimension may be a useful morphometric discriminant in histopathology.* J Pathol, 1992. **166**(4): p. 409-11.
47. Giverso, C. and P. Ciarletta, *On the morphological stability of multicellular tumour spheroids growing in porous media.* Eur Phys J E Soft Matter, 2016. **39**(10): p. 92.
48. Greenspan, H.P., *On the growth and stability of cell cultures and solid tumors.* Journal of Theoretical Biology, 1976. **56**(1): p. 229-242.

49. Landini, G. and J.W. Rippin, *How important is tumour shape? Quantification of the epithelial-connective tissue interface in oral lesions using local connected fractal dimension analysis.* J Pathol, 1996. **179**(2): p. 210-7.
50. Macklin, P., S. Mumenthaler, and J. Lowengrub, *Modeling Multiscale Necrotic and Calcified Tissue Biomechanics in Cancer Patients: Application to Ductal Carcinoma In Situ (DCIS)*, in *Multiscale Computer Modeling in Biomechanics and Biomedical Engineering*, A. Gefen, Editor. 2013, Springer Berlin Heidelberg: Berlin, Heidelberg. p. 349-380.
51. Giverso, C., M. Scianna, and A. Grillo, *Growing Avascular Tumours as Elasto-Plastic Bodies by the Theory of Evolving Natural Configurations.* Mechanics Research Communications, 2015. **68**.
52. Chow, C.L. and Y. Wei, *SECTION 6.4 - Anisotropic Damage*, in *Handbook of Materials Behavior Models*, J. Lemaitre, Editor. 2001, Academic Press: Burlington. p. 421-429.
53. Voyiadjis, G.Z. and M. Yaghoobi, *Chapter 2 - Nonlocal continuum plasticity*, in *Size Effects in Plasticity*, G.Z. Voyiadjis and M. Yaghoobi, Editors. 2019, Academic Press. p. 81-190.
54. Iordan, A., A. Duperray, and C. Verdier, *Fractal approach to the rheology of concentrated cell suspensions.* Physical Review E, 2008. **77**(1): p. 011911.
55. Simo, J.C. and T.J.R. Hughes, *Computational inelasticity*. Interdisciplinary applied mathematics. 1998, New York: Springer. xiv, 392 p.
56. McGinty, B. *Von Mises Stress*. [cited 2019 December 3]; Available from: https://www.continuummechanics.org/vonmisesstress.html.
57. Sciumè, G., et al., *A tumor growth model with deformable ECM.* Physical biology, 2014. **11**(6): p. 065004-065004.